STATISTICS, OPTIMIZATION AND INFORMATION COMPUTING
Stat., Optim. Inf. Comput., Vol. **x**, Month 202x, pp 0–27.
Published online in International Academic Press (www.IAPress.org)

Memory Effects in Eco-Epidemiology: A Dynamical Systems Approach to Fear-Disease-Harvesting Interactions

Siti Nurul Afiyah [1,2], Fatmawati [3,*], Windarto [3], John O. Akanni [4,5]

[1]*Doctoral Program of Mathematics and Natural Science, Faculty of Science and Technology, Universitas Airlangga, Surabaya 60115, Indonesia*
[2] *Informatics Department, Faculty of Technology and Design, Institut Teknologi dan Bisnis Asia, Malang, 65113, Indonesia*
[3]*Department of Mathematics, Faculty of Science and Technology, Universitas Airlangga, Surabaya 60115, Indonesia*
[4]*Department of Mathematics, Saveetha School of Engineering, Saveetha Institute of Medical and Technical Sciences, Saveetha University, Chennai 602105, Tamil Nadu, India*
[5]*Department of Mathematical and Computing Sciences, Koladaisi University, Ibadan, Oyo State*

Abstract
This research proposes a novel fractional-order eco-epidemiological model to investigate prey–predator interactions under the combined effects of fear-induced behavioral changes, disease transmission in predators, and controlled harvesting. Unlike classical integer-order models, our approach employs Caputo fractional derivatives to incorporate memory effects and hereditary traits in ecological processes, offering a more realistic representation of long-term dynamics. We establish the existence, uniqueness, and boundedness of solutions, and analyze the stability of all equilibrium points, including the coexistence state where prey (p) and both susceptible and infected predators ($s + i$) persist. Numerical simulations demonstrate that fear effects increase prey persistence by lowering predation rates, harvesting intensity critically influences system stability, with excessive harvesting driving predator extinction, and fractional-order dynamics reveal memory-dependent transitions not observable in traditional models. Importantly, the fractional order α can be interpreted as an ecological memory index, capturing long-term stress or adaptive responses across generations. These findings provide actionable insights for ecosystem management, particularly in designing harvesting policies that balance biodiversity conservation and disease control. The model's framework is adaptable to empirical data, bridging theoretical ecology and practical conservation strategies.

Keywords Eco-epidemiology, fractional-order models, stability analysis, disease in predator population, fear effect, harvesting.

AMS 2010 subject classifications 92B05, 92D50, 37N25

DOI: 10.19139/soic-2310-5070-2720

1. Introduction

Mathematical biology is a crucial instrument for comprehending the intricate relationships between biological organisms and their environments [1]. One of the most widely used approaches to analyze population dynamics and ecological stability is the predator-prey model. The interactions between organisms in an ecosystem are often influenced by the presence of diseases within the population [2]. The eco-epidemiological approach offers significant insights by merging ecological and epidemiological elements to comprehend the effects of illnesses on interspecies interactions, especially between predators and prey [3]. In natural ecosystems, diseases can significantly affect ecological equilibrium by influencing both prey and predator populations [4].

*Correspondence to: Fatmawati (Email: fatmawati@fst.unair.ac.id). Department of Mathematics, Faculty of Science and Technology, Universitas Airlangga, Surabaya 60115, Indonesia.

ISSN 2310-5070 (online) ISSN 2311-004X (print)

In recent years, numerous scientists have concentrated on analyzing eco-epidemiological models, acknowledging their importance in comprehending the complex interplay between ecology and epidemiology. This approach offers a unique perspective on how diseases influence population dynamics within ecosystems. Research has shown that disease transmission is not solely determined by the characteristics of the infected population but is also shaped by various ecological factors, including species interactions and environmental conditions. In addition, organisms employ adaptive strategies that further influence disease dynamics, such as cannibalism [5, 6, 7], the use of refuge [8, 9, 10], harvesting practices [11, 12, 13, 14, 15], the Allee effect [16, 17], and the fear effect [18, 19, 20, 21, 22, 23, 24, 25]. Additionally, other ecological mechanisms have been identified as contributing factors in shaping disease transmission and population stability [26, 27].

A notable phenomenon in eco-epidemiological systems is the fear effect, which refers to changes in prey behavior triggered by the presence of predators or the risk of disease. This behavioral adaptation influences both individual activity patterns and broader population dynamics. For instance, the fear of predators may drive prey to spend more time in refuges or reduce their foraging activity [24]. These adaptive behaviors help maintain ecological balance, supporting the joint survival of all three species within the system [25].

In ecological systems, the concept of refuge is crucial in influencing predator-prey interactions by offering animals a mechanism for safety from predation [28]. Refuges can take various forms, including physical barriers such as caves, dense vegetation, or deep water, as well as behavioral adaptations like concealment or reduced activity. By lowering predation pressure, these refuges enhance prey survival rates and contribute to the overall stability of the ecosystem. Moreover, the availability and effectiveness of refuges can influence population dynamics, predator foraging behavior, and species coexistence, highlighting their fundamental role in maintaining ecological balance [29, 30].

In addition to the fear effect and the utilization of refuges, another noteworthy event in eco-epidemiological investigations is harvesting, frequently conducted via hunting, capturing, or the extraction of certain species within an ecosystem. This phenomenon has intricate ramifications for population dynamics, particularly in respect to disease transmission and predator-prey interactions. In ecological terms, harvesting can markedly diminish prey populations, hence potentially alleviating predation pressure on them. Intensive harvesting, however, causes the residual prey population to experience stress, rendering them more vulnerable to disease infections due to elevated density in certain regions or compromised immune systems resulting from environmental stressors [31].

These interrelated ecological processes can be clearly illustrated in coral reef ecosystems, where reef fish (prey) seek shelter among coral structures to avoid sharks (predators) [32]. The fear of predation reduces their feeding and reproductive behavior. Simultaneously, sharks may harbor parasites that weaken their predatory capabilities, while refuge availability among reefs shapes how and where these interactions occur [33]. Harvesting pressures from overfishing can further disturb this balance by removing prey or predator species and intensifying stress-driven disease transmission within the ecosystem [34].

These examples highlight the multifaceted and interconnected nature of ecological interactions, where fear effects, refuge use, disease prevalence, and anthropogenic harvesting act simultaneously. Accurately modeling such systems requires an approach capable of capturing not only these interdependencies but also the influence of past events on current dynamics.

Traditional eco-epidemiological models based on integer-order differential equations typically assume that the future state of the system depends solely on its present conditions. However, ecological systems often exhibit *memory effects*, where the evolution of populations is influenced by their entire historical trajectory. A system is deemed memoryless if its state at time t relies exclusively on instantaneous inputs, devoid of any past influence. In contrast, memory-based systems utilize prior input values to determine current outputs [35].

Fractional-order calculus offers a powerful mathematical framework for capturing such memory-dependent behaviors. The use of fractional differential equations enables more accurate representations of complex biological dynamics compared to traditional first-order systems [36]. This approach has gained growing interest in eco-epidemiology, leading to the development of models that incorporate long-term memory and hereditary characteristics [37, 38, 39, 40, 41, 42, 43, 44, 45].

In this study, we adopt a fractional-order modeling approach to better represent the real-world ecological processes described above. By integrating fear effects, refuge dynamics, disease transmission, and harvesting

within a fractional differential equation framework we offer a unified eco-epidemiological model that captures both biological complexity and memory. To the best of our knowledge, this is one of the first models of its kind to address all four factors simultaneously using fractional-order derivatives. Our formulation bridges theoretical insights with ecological realism, contributing to a deeper understanding of predator-prey-disease systems.

2. Model Formulation

We develop an eco-epidemiological model that integrates the combined effects of fear-induced prey behavior, disease transmission in predators, harvesting, and prey refuge. The population is structured into three dynamic compartments, the prey population $P(T)$, predator population $S(T)$ and infected predator population $I(T)$. The model is based on the following ecological assumptions:

1. Predator infection spreads through direct contact among predators, modeled by the bilinear term βSI.
2. Prey grow logistically with intrinsic growth rate r_1 and carrying capacity K, but experience suppression due to fear effects triggered by both predator classes.
3. The fear effect reduces prey reproduction, modeled using a fear function $F(S+I)$.
4. Both predator classes consume prey, influenced by a refuge effect $(1-e)$ and a type-II functional response with half-saturation constant η.
5. Harvesting is applied to prey and susceptible predators, with rates Z_1 and Z_2, respectively.
6. Refuges reduce both predation and harvesting efficiency.
7. Predator mortality includes natural deaths d_1, d_2 and disease-related death d_3, with infected predators assumed to be more fragile.
8. Energy gained from prey is converted to predator growth, modulated by conversion efficiency c.

Based on these assumptions, the classical integer-order system is:

$$\begin{aligned}
\frac{dP}{dT} &= \frac{r_1 P}{1+F(S+I)} - \frac{r_1}{K}P^2 - \frac{V(1-e)PS}{1+\eta(1-e)P} - \frac{V_I(1-e)PI}{1+h(1-e)P} - Z_1(1-e)P,\\
\frac{dS}{dT} &= -d_1 S + \frac{cV(1-e)PS}{1+\eta(1-e)P} - \beta SI - Z_2 S,\\
\frac{dI}{dT} &= \beta SI + \frac{cV_I(1-e)PI}{1+\eta(1-e)P} - (d_2+d_3)I.
\end{aligned} \tag{1}$$

To simplify the system, we apply the nondimensional transformation:

$$p = \frac{P}{K}, \quad s = \frac{S}{K}, \quad i = \frac{I}{K}, \quad t = \beta K T$$

along with the scaled parameters:

$$f = FK, \quad \nu = \frac{V}{\beta K}, \quad \nu_i = \frac{V_I}{\beta K}, \quad r = \frac{r_1}{\beta K}, \quad h = \eta K, \quad z_1 = \frac{Z_1}{\beta K}, \quad z_2 = \frac{Z_2}{\beta K}, \quad d = \frac{d_1}{\beta K}, \quad \gamma = \frac{d_2+d_3}{\beta K}$$

Thus, the dimensionless system becomes:

$$\begin{aligned}
\frac{dp}{dt} &= \frac{rp}{1+f(s+i)} - rp^2 - \frac{\nu(1-e)ps}{1+h(1-e)p} - \frac{\nu_i(1-e)pi}{1+h(1-e)p} - z_1(1-e)p,\\
\frac{ds}{dt} &= -ds + \frac{c\nu(1-e)ps}{1+h(1-e)p} - si - z_2 s,\\
\frac{di}{dt} &= si + \frac{c\nu_i(1-e)pi}{1+h(1-e)p} - \gamma i.
\end{aligned} \tag{2}$$

To provide biological justification, the parameters are summarized in Table 1, including their meaning, plausible ranges, and references from ecological literature. Specific parameter values used in the numerical simulations (Section 4) are chosen within these ranges.

Table 1. Model parameters, biological meaning, plausible ranges, and references.

Parameter	Biological meaning	Plausible range	Reference
r	Intrinsic growth rate of prey	0.5 – 11	[46, 47, 48]
f	Fear coefficient due to predator presence	0.1 – 10	[49, 50]
ν	Predation rate of susceptible predators	0.49 – 0.9	[51]
ν_i	Predation rate of infected predators	0.3 – 0.8	[51]
c	Conversion efficiency of prey into predator growth	0.2 – 0.9	[51, 52]
h	Half-saturation constant	0.002 – 2	[50, 53]
e	Refuge coefficient (proportion of prey in refuge)	0.01 – 0.9	[50]
z_1	Harvesting rate of prey	0.01 – 1.0	[11, 52]
z_2	Harvesting rate of susceptible predators	0.02 – 0.6	[54]
d	Natural mortality of susceptible predators	0.1 – 0.2	[52]
γ	Mortality of infected predators (natural + disease-induced)	0.2 – 1.5	[52]

To account for memory effects in ecological systems, we reformulate the model using Caputo fractional derivatives of order $\alpha \in (0, 1)$. The fractional-order system is written as:

$$\begin{aligned}
{}^{C}D^{\alpha}p(t) &= \frac{rp}{1+f(s+i)} - rp^2 - \frac{\nu(1-e)ps}{1+h(1-e)p} - \frac{\nu_i(1-e)pi}{1+h(1-e)p} - z_1(1-e)p,\\
{}^{C}D^{\alpha}s(t) &= -ds + \frac{c\nu(1-e)ps}{1+h(1-e)p} - si - z_2 s,\\
{}^{C}D^{\alpha}i(t) &= si + \frac{c\nu_i(1-e)pi}{1+h(1-e)p} - \gamma i,
\end{aligned} \tag{3}$$

where ${}^{C}D^{\alpha}$ denotes the Caputo derivative defined by:

$${}^{C}D^{\alpha}f(t) = \frac{1}{\Gamma(n-\alpha)}\int_{t_0}^{t}\frac{f^{(n)}(\tau)}{(t-\tau)^{\alpha+1-n}}d\tau, \quad n = \lceil \alpha \rceil$$

This formulation captures the memory-dependent dynamics of ecological systems and provides a more realistic framework for studying the long-term behavior of interacting species.

3. Mathematical Analysis

In this section, we delineate the fundamental features of the system, including existence, uniqueness, non-negativity, and boundedness of the solution.

3.1. Existence and uniqueness

Define $\Omega := \{(p, s, i) \in \mathbb{R}^3_+ : p, s, i \geq 0, max(p|, |s|, |i|) \leq W\}$ with $W > 0$.

Theorem 3.1
For any non-negative initial conditions (p_0, s_0, i_0), the system (3) has a unique solution $G(t) \in \Omega$.

Proof
It will be shown that the model always has a single solution in $[t_0, \inf) \times \Omega$ if the initial value is given in Ω for every $t \geq t_0$.

Consider $G = (p, s, i)$ and $\bar{G} = (\bar{p}, \bar{s}, \bar{i})$ are the solution of the model (3).
Let $C(G) = (C_1(G), C_2(G)), C_3(G)$, and

$$\begin{aligned}
C_1(G) &= \frac{rp}{1+f(s+i)} - rp^2 - \frac{\nu(1-e)ps}{1+h(1-e)p} - \frac{\nu_i(1-e)pi}{1+h(1-e)p} - z_1(1-e)p,\\
C_2(G) &= -ds + \frac{c\nu(1-e)ps}{1+h(1-e)p} - si - z_2 s,\\
C_3(G) &= si + \frac{c\nu_i(1-e)pi}{1+h(1-e)p} - \gamma i,
\end{aligned}$$

we get,

$$\begin{aligned}
\|C(G) - C(\bar{G})\| &= |C_1(G) - C_1(\bar{G})| + |C_2(G) - C_2(\bar{G})| + |C_3(G) - C_3(\bar{G})|\\
&= \left| \frac{rp}{1+f(s+i)} - rp^2 - \frac{\nu(1-e)ps}{1+h(1-e)p} - \frac{\nu_i(1-e)pi}{1+h(1-e)p} - z_1(1-e)p \right.\\
&\quad \left. - \frac{r\bar{p}}{1+f(\bar{s}+\bar{i})} + r\bar{p}^2 + \frac{\nu(1-e)\bar{p}\bar{s}}{1+h(1-e)\bar{p}} + \frac{\nu_i(1-e)\bar{p}\bar{i}}{1+h(1-e)\bar{p}} + z_1(1-e)\bar{p} \right|\\
&\quad + \left| -ds + \frac{c\nu(1-e)ps}{1+h(1-e)p} - si - z_2 s + d\bar{s} - \frac{c\nu(1-e)\bar{p}\bar{s}}{1+h(1-e)\bar{p}} \right.\\
&\quad \left. + \bar{s}\bar{i} + z_2\bar{s} \right|\\
&\quad + \left| si + \frac{c\nu_i(1-e)pi}{1+h(1-e)p} - \gamma i - \bar{s}\bar{i} - \frac{c\nu_i(1-e)\bar{p}\bar{i}}{1+h(1-e)\bar{p}} + \gamma\bar{i} \right|\\
&\leq r|p-\bar{p}| + rf(\bar{s}+\bar{i})|s-\bar{s}| + rf\bar{p}|p-\bar{p}| + \frac{\nu(1-e)s|p-\bar{p}|}{(1+h(1-e)p)(1+h(1-e)\bar{p})}\\
&\quad + \frac{\nu(1-e)(1+h(1-e)p)\bar{p}|s-\bar{s}|}{(1+h(1-e)p)(1+h(1-e)\bar{p})} + \frac{\nu_i(1-e)i|p-\bar{p}|}{(1+h(1-e)p)(1+h(1-e)\bar{p})}\\
&\quad + \frac{\nu_i(1-e)(1+h(1-e)p)\bar{p}|i-\bar{i}|}{(1+h(1-e)p)(1+h(1-e)\bar{p})} + z_1(1-e)|p-\bar{p}| + (d+z_2)|s-\bar{s}|\\
&\quad + \frac{c\nu(1-e)s|p-\bar{p}|}{(1+h(1-e)p)(1+h(1-e)\bar{p})} + \frac{c\nu(1-e)(1+h(1-e)p)\bar{p}|s-\bar{s}|}{(1+h(1-e)p)(1+h(1-e)\bar{p})}\\
&\quad + 2|si - \bar{s}\bar{i}| + \frac{c\nu_i(1-e)i|p-\bar{p}|}{(1+h(1-e)p)(1+h(1-e)\bar{p})}\\
&\quad + \frac{c\nu_i(1-e)(1+h(1-e)p)\bar{p}|i-\bar{i}|}{(1+h(1-e)p)(1+h(1-e)\bar{p})}\\
&\quad + \gamma|i-\bar{i}|\\
&\leq [r + rf(\bar{s}+\bar{i}) + r(p+\bar{p}) + (1+c)(\nu+\nu_i)(1-e)W + z_1(1-e)]\,|p-\bar{p}|\\
&\quad + [2W + rfW + (1+c)\nu(1-e)(1+h(1-e)W) + d + z_2]\,|s-\bar{s}|\\
&\quad + [2W + rfW + (1+c)\nu_i(1-e)(1+h(1-e)W) + \gamma]\,|i-\bar{i}|\\
&= L_1|p-\bar{p}| + L_2|s-\bar{s}| + L_3|i-\bar{i}|.
\end{aligned}$$

where,

$$\begin{aligned}
L_1 &= r(1 + 2W(f+1) + (1+c)\nu(1-e)W + (1+c)\nu_i(1-e)W + z_1(1-e),\\
L_2 &= 2W + rfW + (1+c)\nu(1-e)(1+h(1-e)W) + (d+z_2),\\
L_3 &= 2W + rfW + (1+c)\nu_i(1-e)(1+h(1-e)W.
\end{aligned}$$

By choosing a positive $L = max(L_1, L_2, L_3)$, we get

$$\|C(G) - C(\bar{G}\| \leq L\|G - \bar{G}\|.$$

Provided that the function $C(G)$ fulfills the Lipschitz condition on the domain Ω, the system (3) possesses a unique solution $G(t) \in \Omega$ for all $t \geq t_0$.

□

3.2. Non-Negativity and Boundedness

Theorem 3.2
For any initial condition $(p(0), s(0), i(0)) \in \mathbb{R}^3_+$, the corresponding solution $(p(t), s(t), i(t))$ of system (3) remains non-negative for all $t > 0$; hence, the non-negative orthant $\mathbb{R}^3_+$ is positively invariant under the dynamics of the system.

Proof
The proof of this theorem relies on Theorem 6 presented by Cresson and Szafranka [55]. In the particular case where $\alpha = 1$, system (3) reduces to the following form:

$$\begin{aligned}
\frac{dp}{dt} &= \frac{rp}{1 + f(s+i)} - rp^2 - \frac{\nu(1-e)ps}{1 + h(1-e)p} - \frac{\nu_i(1-e)pi}{1 + h(1-e)p} - z_1(1-e)p, \\
\frac{ds}{dt} &= -ds + \frac{c\nu(1-e)ps}{1 + h(1-e)p} - si - z_2 s, \\
\frac{di}{dt} &= si + \frac{c\nu_i(1-e)pi}{1 + h(1-e)p} - \gamma i.
\end{aligned}$$

From the first equation,

$$\begin{aligned}
\frac{dp}{dt} &= \frac{rp}{1 + f(s+i)} - rp^2 - \frac{\nu(1-e)ps}{1 + h(1-e)p} - \frac{\nu_i(1-e)pi}{1 + h(1-e)p} - z_1(1-e)p \\
\frac{dp}{dt} &= p\left(\frac{r}{1 + f(s+i)} - rp - \frac{\nu(1-e)s}{1 + h(1-e)p} - \frac{\nu_i(1-e)i}{1 + h(1-e)p} - z_1(1-e)\right) \\
\frac{dp}{p} &= \left(\frac{r}{1 + f(s+i)} - rp - \frac{\nu(1-e)s}{1 + h(1-e)p} - \frac{\nu_i(1-e)i}{1 + h(1-e)p} - z_1(1-e)\right) dt \\
p(t) &= p(0) \\
&\quad \exp\left\{\int_0^t \left(\frac{r}{1 + f(s(\tau)+i(\tau))} - rp(\tau) - \frac{\nu(1-e)s(\tau)}{1 + h(1-e)p(\tau)} - \frac{\nu_i(1-e)i(\tau)}{1 + h(1-e)p(\tau)} - z_1(1-e)\right) d\tau\right\} \\
&\quad \geq 0\}.
\end{aligned}$$

From the second equation,

$$\begin{aligned}
\frac{ds}{dt} &= -ds + \frac{c\nu(1-e)ps}{1+h(1-e)p} - si - z_2 s \\
\frac{ds}{dt} &= s\left(-d + \frac{c\nu(1-e)s}{1+h(1-e)p} - i - z_2\right) \\
\frac{ds}{s} &= \left(-d + \frac{c\nu(1-e)s}{1+h(1-e)p} - i - z_2\right) dt \\
\ln(s) - \ln s(0) &= \int_0^t \left(-d + \frac{c\nu(1-e)s(\tau)}{1+h(1-e)p(\tau)} - i(\tau) - z_2\right) d\tau \\
\ln(s) &= \int_0^t \left(-d + \frac{c\nu(1-e)s(\tau)}{1+h(1-e)p(\tau)} - i(\tau) - z_2\right) d\tau + \ln s(0) \\
s(t) &= s(0)\exp\left\{\int_0^t \left(-d + \frac{c\nu(1-e)s(\tau)}{1+h(1-e)p(\tau)} - i(\tau) - z_2\right) d\tau\right\} \geq 0.
\end{aligned}$$

From the third equation,

$$\begin{aligned}
\frac{di}{dt} &= si + \frac{c\nu_i(1-e)pi}{1+h(1-e)p} - \gamma i \\
\frac{di}{dt} &= i\left(s + \frac{c\nu_i(1-e)p}{1+h(1-e)p} - \gamma\right) \\
\frac{di}{i} &= \left(s + \frac{c\nu_i(1-e)p}{1+h(1-e)p} - \gamma\right) dt \\
\ln(i) - \ln i(0) &= \int_0^t \left(s(\tau) + \frac{c\nu_i(1-e)p(\tau)}{1+h(1-e)p(\tau)} - \gamma\right) d\tau \\
\ln(i) &= \int_0^t \left(s(\tau) + \frac{c\nu_i(1-e)p(\tau)}{1+h(1-e)p(\tau)} - \gamma\right) d\tau + \ln i(0) \\
i(t) &= i(0)\exp\left\{\int_0^t \left(s(\tau) + \frac{c\nu_i(1-e)p(\tau)}{1+h(1-e)p(\tau)} - \gamma\right) d\tau\right\} \geq 0.
\end{aligned}$$

Given that $\vec{f}(\vec{x}(t))$ adheres to Local Lipschitz conditions, with $p(t) \geq 0$, $s(t) \geq 0$, and $i(t) \geq 0$ for $\alpha = 1$ and non-negative initial values, it follows from Theorem 6 by Cresson and Szafranka [55] that model (3) possesses a non-negative solution. □

Theorem 3.3
For any initial condition $(p(0), s(0), i(0)) \in \mathbb{R}^3_+$, the corresponding solution $(p(t), s(t), i(t))$ of system (3) remains uniformly bounded on the interval $[0, \infty)$.

Proof
Let the function be defined as $N(t) = p(t) + \frac{1}{c}s(t) + \frac{1}{c}i(t)$; consequently, we obtain

$${}^C D^\alpha N(t) = {}^C D^\alpha p(t) + \frac{1}{c}{}^C D^\alpha s(t) + \frac{1}{c}{}^C D^\alpha i(t).$$

For each positive constant ρ, it holds that

$$\begin{aligned}
{}^{C}D^{\alpha}N(t)+\rho N(t) &= \frac{rp}{1+f(s+i)} - rp^2 - \frac{\nu(1-e)ps}{1+h(1-e)p} - \frac{\nu_i(1-e)pi}{1+h(1-e)p} - z_1(1-e)p \\
&+ \frac{1}{c}(-ds + \frac{c\nu(1-e)ps}{1+h(1-e)p} - si - z_2 s) + \frac{1}{c}(si + \frac{c\nu_i(1-e)pi}{1+h(1-e)p} - \gamma i) \\
&+ \rho(p + \frac{1}{c}s + \frac{1}{c}i) \\
&= (\frac{rp}{1+f(s+i)} - z_1(1-e) + \rho)p - rp^2 + \frac{(\rho - d - z_2)}{c}s + \frac{\rho-\gamma}{c}i.
\end{aligned}$$

By choosing $\rho < min(d+z_2, \gamma)$

$$\begin{aligned}
{}^{C}D^{\alpha}N(t)+\rho N(t) &\leq rp - z_1(1-e)p + \rho p - rp^2 \\
&= -rp^2 + (r - z_1(1-e) + \rho)p \\
&\leq \frac{1}{4r}(r - z_1(1-e) + \rho)^2.
\end{aligned}$$

Utilizing the Fractional Comparison Principle [56], we obtain

$$N(t) \leq \left(N(0) - \frac{1}{4r}(r - z_1(1-e) + \rho)^2\right) E_{\alpha}(-\rho(t)^{\alpha}) + \frac{1}{4r}(r - z_1(1-e) + \rho)^2.$$

As $t \to \infty$, $E_{\alpha}(-\rho(t)^{\alpha}) \to 0$, hence $N(t) \to \frac{1}{4r}(r - z_1(1-e) + \rho)^2$ as $t \to \infty$. In other words, every solution of the system (3) that begins in $\mathbb{R}^3_+$ continues in the region σ, where

$$\sigma = \left((p,s,i) \in \mathbb{R}^3_+ : p + \frac{1}{c}s + \frac{1}{c}i \leq \frac{1}{4r}(r - z_1(1-e) + \rho)^2 + \epsilon, \epsilon > 0\right).$$

□

3.3. Equilibrium Points

The fractional-order system (3) admits the following equilibrium points:

1. The trivial equilibrium $E_0 = (0,0,0)$, which always exists.
2. The predator-free equilibrium $E_1 = \left(\frac{r - z_1(1-e)}{r}, 0, 0\right)$, which exists provided that $r > z_1(1-e)$.
3. The susceptible-predator-free equilibrium $E_2 = (p_2, 0, i_2)$, where

$$p_2 = \frac{\gamma}{c\nu_i(1-e) - \gamma h(1-e)}, \quad i_2 = \frac{-A_1 + \sqrt{A_1^2 - 4A_0A_2}}{2A_0}.$$

   where

$$\begin{aligned}
A_0 &= \nu_i(1-e)f, \\
A_1 &= \nu_i(1-e) + z_1(1-e)^2 hp_2 f + z_1(1-e)f + rp_2 f + rp_2^2 fh(1-e), \\
A_2 &= rp_2 + h(1-e)p_2^2 r + z_1(1-e) + z_1(1-e)^2 hp_2 - r - rh(1-e)p_2.
\end{aligned}$$

   The susceptible predator free equilibrium point $E_2(p_2, 0, i_2)$ exist if $c\nu_i > \gamma h$ and $A_2 < 0$.
4. The disease-free equilibrium point $E_3(p_3, s_3, 0)$, where $p_3 = \frac{d+z_2}{c\nu(1-e) - (d+z_2)h(1-e)}$, and $s_3 = \frac{-B_1 + \sqrt{B_1^2 - 4B_0B_2}}{2B_0}$, where

$$\begin{aligned}
B_0 &= \nu(1-e)f, \\
B_1 &= \nu(1-e) + z_1(1-e)^2 hp_3 f + z_1(1-e)f + rp_3 f + rp_3^2 fh(1-e), \\
B_2 &= rp_3 + h(1-e)p_3^2 r + z_1(1-e) + z_1(1-e)^2 hp_3 - r - rh(1-e)p_3,
\end{aligned}$$

The existence of the disease-free equilibrium point $E_3 = (p_3, s_3, 0)$ requires that $c\nu > (d + z_2)h$ and $B_2 < 0$.

5. The coexistence equilibrium point $E^*(p^*, s^*, i^*)$, where $s^* = \gamma - \frac{c\nu_i(1-e)p^*}{1+h(1-e)p^*}$, $i^* = -(d + z_2) + \frac{c\nu(1-e)p^*}{1+h(1-e)p^*}$. Substituting s^* and i^* in prey nullcline equation gives the following polinomial equation,

$$C_0 + C_1 p^* + C_2 {p^*}^2 + C_3 {p^*}^3 + C_4 {p^*}^4 = 0 \tag{4}$$

where C_0, C_1, C_2, C_3, C_4 are given in the Appendix. s^* and i^* are uniquely defined if p^* is a solution of the quartic polinomial equation (4). To determine the coexistence equilibrium point, it is required to find at least one positive root of equation (4). The equation (4) possesses a maximum of four complex roots. Assume the existence of one pair of complex roots, specifically θ and its conjugate θ^*. The following quadratic equation

$$P^2 + \sigma_1 P + \sigma_2 = (P - \theta)(P - \theta^*) = P^2 - 2Re(\theta)P + |\theta|^2$$

is created by a conjugate pair wherein $\sigma_1 = -2Re(\theta), \sigma_2 = |\theta|^2$. Let us assume that the equation (4) possesses two real roots, denoted as p_1^* and p_2^*, such that their sum is $p_1^* + p_2^* = -\vartheta_1$ and their product is $p_1^* p_2^* = \vartheta_2$. Thus, the factorization of equation (4) is as follows:

$$\begin{aligned} C_0 + C_1 p^* + C_2 {p^*}^2 + C_3 {p^*}^3 + C_4 {p^*}^4 &= C_4(P^2 + \sigma_1 P + \sigma_2)(P^2 + \vartheta_1 P + \vartheta_2) \\ &= C_4[P^4 + (\sigma_1 + \vartheta_1)P^3 + (\sigma_2 + \vartheta_2 + \sigma_1\vartheta_1)P^2 \\ &+ (\sigma_1\vartheta_2 + \sigma_2\vartheta_1)P + \sigma_2\vartheta_2]. \end{aligned}$$

By equating coefficients on both sides, we ascertain that

$$\vartheta_1 = \frac{C_3}{C_4} + 2Re(\theta), \vartheta_2 = \frac{C_0}{C_4|\theta|^2}.$$

We will now examine the two potential scenarios that may occur.
Scenario 1: If $\vartheta_2 > 0$, specifically, if $z_1(1-e)(1+fA) > r + \nu_i(1-e)(d+z_2)$, then both real roots are positive if the following criteria are met: $\vartheta_1 < 0$ and $\vartheta_1^2 - 4\vartheta_2 > 0$. Consequently, there are two positive real roots.

$$p_1^* = \frac{-\vartheta_1 + \sqrt{\vartheta_1^2 - 4\vartheta_2}}{2}, p_2^* = \frac{-\vartheta_1 - \sqrt{\vartheta_1^2 - 4\vartheta_2}}{2}.$$

Scenario 2: If $\vartheta_2 < 0$, that is, if $z_1(1-e)(1+fA) < r + \nu_i(1-e)(d+z_2)$, then one root is evidently positive, fulfilling the above conditions.
Consequently, the condition for the existence of the coexistence equilibrium point $E^*(p^*, s^*, i^*)$ is given by $\gamma > d + z_2$, $\frac{c\nu(1-e)p^*}{1+h(1-e)p^*} > d + z_2$, $\gamma > \frac{c\nu_i(1-e)p^*}{1+h(1-e)p^*}$, and $z_1(1-e)(1+fA) < r + \nu_i(1-e)(d+z_2)$.

3.4. Local Stability

To investigate the local stability of system (3), we apply the classical linearization technique. The corresponding Jacobian matrix is expressed as:

$$\mathbf{J}(p, s, i) = \begin{bmatrix} N_{11} & N_{12} & N_{13} \\ N_{21} & N_{22} & N_{23} \\ N_{31} & N_{32} & N_{33} \end{bmatrix}$$

where,

$$
\begin{aligned}
N_{11} &= \frac{r}{1+f(s+i)} - 2rp - \frac{\nu(1-e)s}{(1+h(1-e)p)^2} - \frac{\nu_i(1-e)i}{(1+h(1-e)p)^2} - z_1(1-e),\\
N_{12} &= -\frac{rpf}{(1+f(s+i))^2} - \frac{\nu(1-e)p}{1+h(1-e)p},\\
N_{13} &= -\frac{rpf}{(1+f(s+i))^2} - \frac{\nu_i(1-e)p}{1+h(1-e)p},\\
N_{21} &= \frac{c\nu(1-e)s}{(1+h(1-e)p)^2},\\
N_{22} &= -d + \frac{c\nu(1-e)p}{1+h(1-e)p} - i - z_2,\\
N_{23} &= -s,\\
N_{31} &= \frac{c\nu_i(1-e)i}{(1+h(1-e)p)^2},\\
N_{32} &= i,\\
N_{33} &= s + \frac{c\nu_i(1-e)p}{1+h(1-e)p} - \gamma.
\end{aligned}
$$

Theorem 3.4
The trivial equilibrium $E_0 = (0,0,0)$ exhibits asymptotic stability when the condition $r < z_1(1-e)$ holds. If this condition is not satisfied, the equilibrium becomes unstable.

Proof
At the trivial equilibrium $E_0(0,0,0)$, the Jacobian matrix of system (3) takes the diagonal form:

$$
J(E_0) = \begin{bmatrix} r - z_1(1-e) & 0 & 0 \\ 0 & -d - z_2 & 0 \\ 0 & 0 & -\gamma \end{bmatrix},
$$

with characteristic equation $\det(J(E_0) - \lambda I) = 0$ yielding explicit eigenvalues:

$$
\begin{aligned}
\lambda_1 &= r - z_1(1-e),\\
\lambda_2 &= -d - z_2 < 0,\\
\lambda_3 &= -\gamma < 0.
\end{aligned}
$$

Case 1: When $r < z_1(1-e)$, all eigenvalues are negative:

$$
|\arg(\lambda_i)| = \pi > \frac{\alpha\pi}{2}, \quad \text{for } i = 1,2,3.
$$

By the fractional-order stability criterion, E_0 is asymptotically stable.

Case 2: For $r > z_1(1-e)$, we have:

$$
\begin{aligned}
|\arg(\lambda_1)| &= 0 < \frac{\alpha\pi}{2},\\
|\arg(\lambda_2)| &= |\arg(\lambda_3)| = \pi > \frac{\alpha\pi}{2}.
\end{aligned}
$$

This eigenvalue configuration (one unstable and two stable modes) makes E_0 a saddle point, hence unstable. □

Theorem 3.5
The predator free equilibrium point $E_1(\frac{r-z_1(1-e)}{r}, 0, 0)$ is stable if $\frac{c\nu(1-e)(r-z_1(1-e))}{r+h(1-e)(r-z_1(1-e))} < d + z_2$ and $\frac{c\nu_i(1-e)(r-z_1(1-e))}{r+h(1-e)(r-z_1(1-e))} < \gamma$, while saddle point if $\frac{c\nu(1-e)(r-z_1(1-e))}{r+h(1-e)(r-z_1(1-e))} > d + z_2$ and $\frac{c\nu_i(1-e)(r-z_1(1-e))}{r+h(1-e)(r-z_1(1-e))} > \gamma$.

Proof
The Jacobian matrix for $E_1(\frac{r-z_1(1-e)}{r}, 0, 0)$ is

$$\mathbf{J}(E_1) = \begin{bmatrix} N_{11} & N_{12} & N_{13} \\ 0 & N_{22} & 0 \\ 0 & 0 & N_{33} \end{bmatrix}.$$

where,

$$\begin{aligned}
N_{11} &= -r + z_1(1-e), \\
N_{12} &= -(r - z_1(1-e))f - \frac{\nu(1-e)(r - z_1(1-e))}{r - h(1-e)(r - z_1(1-e))}, \\
N_{13} &= -(r - z_1(1-e))f - \frac{\nu_i(1-e)(r - z_1(1-e))}{r - h(1-e)(r - z_1(1-e))}, \\
N_{22} &= -d + \frac{c\nu(1-e)(r - z_1(1-e))}{r - h(1-e)(r - z_1(1-e))} - z_2, \\
N_{33} &= \frac{c\nu_i(1-e)(r - z_1(1-e))}{r - h(1-e)(r - z_1(1-e))} - \gamma,
\end{aligned}$$

with characteristic equation $\det(J(E_1) - \lambda I) = 0$ yielding explicit eigenvalues: $\lambda_1 = -r + z_1(1-e)$, $\lambda_2 = -d + \frac{c\nu(1-e)(r-z_1(1-e))}{r+h(1-e)(r-z_1(1-e))} - z_2$ and $\lambda_3 = \frac{c\nu_i(1-e)(r-z_1(1-e))}{r+h(1-e)(r-z_1(1-e))} - \gamma$. Given that $r > z_1(1-e)$ ensures the existence of the equilibrium point E_1, it follows that λ_1 is always a negative real number. Consequently, $|\arg(\lambda_1)| = \pi > \frac{\alpha\pi}{2}$. If $\frac{c\nu(1-e)(r-z_1(1-e))}{r+h(1-e)(r-z_1(1-e))} < d + z_2$, $\lambda_2 < 0$. Thus $|arg(\lambda_2)| = \pi > \frac{\alpha\pi}{2}$. If $\frac{c\nu_i(1-e)(r-z_1(1-e))}{r+h(1-e)(r-z_1(1-e))} < \gamma$, $\lambda_3 < 0$. Thus $|arg(\lambda_3)| = \pi > \frac{\alpha\pi}{2}$. It follows that, under the specified condition, the predator-free equilibrium E_1 is locally asymptotically stable. Otherwise, if $\frac{c\nu(1-e)(r-z_1(1-e))}{r+h(1-e)(r-z_1(1-e))} > d + z_2$, $\lambda_2 > 0$. Thus $|arg(\lambda_2)| = 0 < \frac{\alpha\pi}{2}$. If $\frac{c\nu_i(1-e)(r-z_1(1-e))}{r+h(1-e)(r-z_1(1-e))} > \gamma$, $\lambda_3 > 0$. Therefore, since $|\arg(\lambda_3)| = 0 < \frac{\alpha\pi}{2}$, the predator-free equilibrium point $E_1$is classified as a saddle point.

□

Theorem 3.6
Suppose that:

$$\begin{aligned}
\Delta &= \left(\frac{r}{1+fi_2} - 2rp_2 - \frac{\nu_i(1-e)i_2}{(1+h(1-e)p_2)^2} - z_1(1-e) \right)^2 \\
&\quad - 4\left(\frac{rfc\nu_i(1-e)p_2i_2}{(1+fi_2)^2(1+h(1-e)p_2)^2} + \frac{c\nu_i^2(1-e)^2p_2i_2}{(1+h(1-e)p_2)^3}) \right), \\
\alpha^* &= \frac{2}{\pi} tan^{-1} \left(\frac{\sqrt{|\Delta|}}{\frac{r}{1+fi_2} - 2rp_2 - \frac{\nu_i(1-e)i_2}{(1+h(1-e)p_2)^2} - z_1(1-e)} \right)
\end{aligned}$$

The susceptible predator free equilibrium point $E_2(p_2, 0, i_2)$ is locally asymptotically stable if $\frac{c\nu(1-e)p_2}{(1+h(1-e)p_2)} < d + i_2 + z_2$ and

1. $\frac{r}{1+fi_2} - 2rp_2 - \frac{\nu_i(1-e)i_2}{(1+h(1-e)p_2)^2} - z_1(1-e) < 0$, or;
2. $\frac{r}{1+fi_2} - 2rp_2 - \frac{\nu_i(1-e)i_2}{(1+h(1-e)p_2)^2} - z_1(1-e) > 0, \Delta < 0$ and $\alpha < \alpha^*$

Proof
The Jacobian matrix for $E_2(p_2, 0, i_2)$ is

$$\mathbf{J}(E_2) = \begin{bmatrix} K_{11} & K_{12} & K_{13} \\ 0 & K_{22} & 0 \\ K_{31} & K_{32} & 0 \end{bmatrix}.$$

where,

$$
\begin{aligned}
K_{11} &= \frac{r}{1+fi_2} - 2rp_2 - \frac{\nu_i(1-e)i_2}{(1+h(1-e)p_2)^2} - z_1(1-e),\\
K_{12} &= -\frac{rp_2 f}{(1+fi_2)^2} - \frac{\nu(1-e)p_2}{1+h(1-e)p_2},\\
K_{13} &= -\frac{rp_2 f}{(1+fi_2)^2} - \frac{\nu_i(1-e)p_2}{1+h(1-e)p_2},\\
K_{22} &= -(d+i_2+z_2) + \frac{c\nu(1-e)p_2}{1+h(1-e)p_2},\\
K_{31} &= \frac{c\nu_i(1-e)i_2}{(1+h(1-e)p_2)^2},\\
K_{32} &= i_2.
\end{aligned}
$$

The Jacobian matrix evaluated at the equilibrium point $J(E_2)$ has three eigenvalues. The first eigenvalue is explicitly given by $\lambda_1 = -(d+i_2+z_2) + \frac{c\nu(1-e)p_2}{1+h(1-e)p_2}$ and the other two eigenvalues are the solution of $\lambda_{2,3} = \frac{\frac{r}{1+fi_2} - 2rp_2 - \frac{\nu_i(1-e)i_2}{(1+h(1-e)p_2)^2} - z_1(1-e)}{2} \pm \frac{\sqrt{\Delta}}{2}$. If $\lambda_1 = \frac{c\nu(1-e)p_2}{1+h(1-e)p_2} < d+i_2+z_2$, then $|arg(\lambda_1)| = \pi > \frac{\alpha\pi}{2}$. Furthermore, if $\frac{r}{1+fi_2} - 2rp_2 - \frac{\nu_i(1-e)i_2}{(1+h(1-e)p_2)^2} - z_1(1-e) < 0$, then $|arg(\lambda_{2,3})| = \pi > \frac{\alpha\pi}{2}$. If $\frac{r}{1+fi_2} - 2rp_2 - \frac{\nu_i(1-e)i_2}{(1+h(1-e)p_2)^2} - z_1(1-e) > 0$ and $e < 0$, then $\lambda_{2,3}$ is a pair of complex eigenvalues. Thus, $|arg(\lambda_{2,3})| = \pi > \frac{\alpha\pi}{2}$ was achieved if $\alpha < \alpha^*$. Using the Matignon's condition (Theorem 5), the theorem is completely proven. □

Theorem 3.7
Suppose that:

$$
\begin{aligned}
\omega_1 &= -\frac{r}{1+fs_3} + 2rp_3 + \frac{\nu(1-e)s_3}{(1+h(1-e)p_3)^2} + z_1(1-e),\\
\omega_2 &= \left(\frac{rp_3 f}{(1+fs_3)^2} + \frac{\nu(1-e)p_3}{1+h(1-e)p_3}\right)\left(\frac{c\nu(1-e)s_3}{(1+h(1-e)p_3)^2}\right)
\end{aligned}
$$

The disease free equilibrium point $E_3(p_3, s_3, 0)$ is locally asymptotically stable if

1. $s_3 + \frac{c\nu_i(1-e)p_3}{1+h(1-e)p_3} < \gamma, \omega_1 > 0$ and $\omega_2 > 0$, or;
2. $s_3 + \frac{c\nu_i(1-e)p_3}{1+h(1-e)p_3} < \gamma, \omega_1 < 0, 4\omega_2 > \omega_1^2$, and $tan^{-1}(\frac{\sqrt{4\omega_2 - \omega_1^2}}{\omega_1}) > \frac{\alpha\pi}{2}$.

Proof
The Jacobian matrix for $E_3(p_3, s_3, 0)$ is

$$
\mathbf{J}(E_3) = \begin{bmatrix} L_{11} & L_{12} & L_{13} \\ L_{21} & 0 & L_{23} \\ 0 & 0 & L_{33} \end{bmatrix}.
$$

where,

$$
\begin{aligned}
L_{11} &= \frac{r}{1+fs_3} - 2rp_3 - \frac{\nu(1-e)s_3}{(1+h(1-e)p_3)^2} - z_1(1-e),\\
L_{12} &= -\frac{rp_3 f}{(1+fs_3)^2} - \frac{\nu(1-e)p_3}{1+h(1-e)p_3},\\
L_{13} &= -\frac{rp_3 f}{(1+fs_3)^2} - \frac{\nu_i(1-e)p_3}{1+h(1-e)p_3},\\
L_{21} &= \frac{c\nu(1-e)s_3}{(1+h(1-e)p_3)^2},\\
L_{23} &= -s_3,\\
L_{33} &= s_3 + \frac{c\nu_i(1-e)p_3}{1+h(1-e)p_3} - \gamma.
\end{aligned}
$$

One of the eigenvalues of the Jacobian matrix $J(E_3)$ is $\lambda_1 = s_3 + \frac{c\nu_i(1-e)p_3}{1+h(1-e)p_3} - \gamma$ and the other two eigenvalues are the solution of $\lambda^2 + \omega_1\lambda + \omega_2 = 0$. If $s_3 + \frac{c\nu_i(1-e)p_3}{1+h(1-e)p_3} < \gamma$, then $|arg(\lambda_1)| = \pi > \frac{\alpha\pi}{2}$. Furthermore, using the Routh-Hurwitz criteria for a fractional order dynamic system, the two other eigenvalues satisfy $|arg(\lambda)| = \pi > \frac{\alpha\pi}{2}$ if

1. $\omega_1 > 0$ and $\omega_2 > 0$ or,
2. $\omega_1 < 0, 4\omega_2 > \omega_1^2$, and $tan^{-1}(\frac{\sqrt{4\omega_2 - \omega_1^2}}{\omega_1}) > \frac{\alpha\pi}{2}$.

Therefore, $E_3(p_3, s_3, 0)$ is locally asymptotically stable if conditions (1) or (2) satisfied. □

Theorem 3.8
Suppose that:

$$
\begin{aligned}
\varphi_1 &= -M_{11},\\
\varphi_2 &= -M_{23}M_{32} - M_{12}M_{21} - M_{13}M_{31},\\
\varphi_2 &= M_{11}M_{23}M_{32} - M_{12}M_{23}M_{31} - M_{13}M_{21}M_{32},
\end{aligned}
$$

The coexistence equilibrium point $E^*(p^*, s^*, i^*)$ is locally asymptotically stable if $\varphi_1 > 0, \varphi_3 > 0$, and $\varphi_1\varphi_2 > \varphi_3$.

Proof
The Jacobian matrix for $E^*(p^*, s^*, i^*)$ is

$$
\mathbf{J}(E^*) = \begin{bmatrix} M_{11} & M_{12} & M_{13} \\ M_{21} & 0 & M_{23} \\ M_{31} & M_{32} & 0 \end{bmatrix}.
$$

where,

$$
\begin{aligned}
M_{11} &= \frac{r}{1+f(s^*+i^*)} - 2rp^* - \frac{\nu(1-e)s^*}{(1+h(1-e)p^*)^2} - \frac{\nu_i(1-e)i^*}{(1+h(1-e)p^*)^2} - z_1(1-e),\\
M_{12} &= -\frac{rp^*f}{(1+f(s^*+i^*))^2} - \frac{\nu(1-e)p^*}{1+h(1-e)p^*},\\
M_{13} &= -\frac{rp^*f}{(1+f(s^*+i^*))^2} - \frac{\nu_i(1-e)p^*}{1+h(1-e)p^*},\\
M_{21} &= \frac{c\nu(1-e)s^*}{(1+h(1-e)p^*)^2},\\
M_{23} &= -s^*,\\
M_{31} &= \frac{c\nu_i(1-e)i^*}{(1+h(1-e)p^*)^2},\\
M_{32} &= i^*.
\end{aligned}
$$

The corresponding characteristic equation is

$$\lambda^3 + \varphi_1\lambda^2 + \varphi_2\lambda + \varphi_3 = 0,$$

where

$$
\begin{aligned}
\varphi_1 &= -M_{11},\\
\varphi_2 &= -M_{23}M_{32} - M_{12}M_{21} - M_{13}M_{31},\\
\varphi_2 &= M_{11}M_{23}M_{32} - M_{12}M_{23}M_{31} - M_{13}M_{21}M_{32}.
\end{aligned}
$$

By the Routh–Hurwitz stability criterion, the coexistence equilibrium $E^*(p^*, s^*, i^*)$ is locally asymptotically stable if and only if $\varphi_1 > 0,\ \varphi_3 > 0$, and $\varphi_1\varphi_2 > \varphi_3$.

□

3.5. Global Stability

Theorem 3.9
The equilibrium point $E_0(0,0,0)$ is said to be globally stable if it satisfies $r < z_1(1-e)$.

Proof
Let us define a Lyapunov function to analyze the stability of the system,

$$V_0(p,s,i) = p + \frac{1}{c}s + \frac{1}{c}i,$$

In accordance with Lemma 3.1 from Vargas De León [57], it follows that we can express the system as follows:

$$
\begin{aligned}
{}^C D^\alpha V_0 &\le {}^C D^\alpha p + \frac{1}{c}{}^C D^\alpha s + \frac{1}{c}{}^C D^\alpha i,\\
&= \left(\frac{rp}{1+f(s+i)} - rp^2 - \frac{\nu(1-e)ps}{1+h(1-e)p} - \frac{\nu_i(1-e)pi}{1+h(1-e)p} - z_1(1-e)p\right)\\
&+ \frac{1}{c}\left(-ds + \frac{c\nu(1-e)ps}{1+h(1-e)p} - si - z_2 s\right) + \frac{1}{c}\left(si + \frac{c\nu_i(1-e)pi}{1+h(1-e)p} - \gamma i\right),\\
&= \frac{rp}{1+f(s+i)} - rp^2 - z_1(1-e)p - \frac{ds}{c} - \frac{z_2}{c} - \frac{\gamma}{c},\\
&\le [r - z_1(1-e)]\, p.
\end{aligned}
$$

It is evident that ${}^{C}D^{\alpha}V_0 \leq 0$ when $r < z_1(1-e)$, indicating that the Lyapunov function $V_0(p,s,i)$ satisfies the condition for global stability. Therefore, we conclude that the equilibrium point E_0 is globally asymptotically stable under the condition $r < z_1(1-e)$.

□

Theorem 3.10
The coexistence equilibrium point $E^*(p^*, s^*, i^*)$ is globally asymptotically stable.

Proof
Let us examine the following Lyapunov function, which satisfies the condition of positive definiteness:

$$V_1(p,s,i) = [p - p^* - p^* ln\frac{p}{p^*}] + [s - s* - s* ln\frac{s}{s^*}] + [i - i* - i* ln\frac{i}{i^*}]$$

According to Lemma 3.1 in [57], it follows that:

$$\begin{aligned}
{}^{C}D^{\alpha}V_1(p,s,i) &\leq \left[\frac{p-p^*}{p}\right] {}^{C}D^{\alpha}p + \left[\frac{s-s^*}{s}\right] {}^{C}D^{\alpha}s + \left[\frac{i-i^*}{i}\right] {}^{C}D^{\alpha}i, \\
&= [p-p^*]\left(\frac{r}{1+f(s+i)} - rp - \frac{\nu(1-e)s}{1+h(1-e)p} - \frac{\nu_i(1-e)i}{1+h(1-e)p} - z_1(1-e)\right) \\
&+ [s-s^*]\left(-d + \frac{c\nu(1-e)p}{1+h(1-e)p} - i - z_2\right) + [i-i^*]\left(s + \frac{c\nu_i(1-e)p}{1+h(1-e)p} - \gamma\right), \\
&\leq -(p-p^*)(-r\left(\frac{1}{1+f(s+i)} - \frac{1}{1+f(s^*+i^*)}\right) + r(p-p^*) \\
&+ \nu(1-e)\left(\frac{s}{1+h(1-e)p} - \frac{s^*}{1+h(1-e)p^*}\right) \\
&+ \nu_i(1-e)\left(\frac{i}{1+h(1-e)p} - \frac{i^*}{1+h(1-e)p^*}\right)) - (s-s^*) \\
&(-c\nu(1-e)\left(\frac{p}{1+h(1-e)p} - \frac{p^*}{1+h(1-e)p^*}\right) + (i-i^*)) \\
&- (i-i^*)((s-s^*) - c\nu_i(1-e)\left(\frac{p}{1+h(1-e)p} - \frac{p^*}{1+h(1-e)p^*}\right)).
\end{aligned}$$

It is obvious that $V_1(p,s,i) \leq 0$. We find out that the coexistence equilibrium point $E^*(p^*, s^*, i^*)$ is globally asymptotically stable.

□

4. Numerical Simulation and Discussion

To support and visualize the analytical findings, a series of numerical simulations were conducted for different parameter sets representing distinct ecological scenarios. The specific parameter values and their corresponding interpretations are summarized in Table 1. For reference, these parameter sets are used consistently throughout this section: Set 1 corresponds to the trivial equilibrium (E_0), Set 2 to the predator-free equilibrium (E_1), Set 3 to the susceptible predator-free equilibrium (E_2), Set 4 to the disease-free equilibrium (E_3), and Set 5 to the interior coexistence equilibrium (E^*). In addition, Set 6 is introduced to explore the combined effects of refuge proportion and memory (fractional order α) on the system's stability. Together, these simulations provide a comprehensive numerical validation of the analytical results and offer deeper ecological insights into how fear, disease, harvesting, and memory shape the long-term dynamics of the system.

Table 2. Parameter values used in the numerical simulations (Sets 1–5).

Set	r	f	ν	ν_i	c	h	e	z_1	z_2	d	γ	Figure
1	0.5	2.0	0.49	0.3	0.2	0.05	0.05	0.6	0.6	0.2	0.3	Figure 1
2	0.5	2.0	0.49	0.3	0.2	0.05	0.05	0.2	0.6	0.2	0.3	Figure 2
3	0.7	2.0	0.9	0.8	0.9	0.1	0.2	0.5	0.4	0.1	0.2	Figure 3
4	0.7	2.0	0.9	0.8	0.9	0.1	0.7	1.0	0.02	0.1	0.6	Figure 4
5	1.5	1.5	0.9	0.5	0.9	0.4	0.2	0.1	0.02	0.1	0.6	Figure 5, Figure 6
6	10	0	0.9	0.8	0.9	0.1	0.8	0.1	1	0.02	0.6	Figure 7, Figure 8

This section presents numerical simulations of the fractional-order eco-epidemiological model (3) to demonstrate the theoretical results derived earlier. The simulations are carried out using the Adams–Bashforth–Moulton predictor–corrector method [58], which provides accurate approximate solutions for fractional-order differential equations. Since no empirical data are currently available for this model, the parameter values listed in Table 2 were selected within plausible biological ranges (see Table 1) and adjusted to illustrate different ecological scenarios such as high harvesting pressure and varying refuge proportions.

The simulations are organized to progressively illustrate the dynamical behavior of the system under different ecological conditions. We begin with the simplest case where all populations vanish, and then gradually include the effects of prey recovery, disease transmission, and coexistence of multiple species. Finally, we examine how refuge and memory jointly influence system stability. This structured approach allows each simulation to highlight a specific ecological mechanism while collectively demonstrating the consistency between analytical predictions and numerical outcomes.

Simulation 1: Trivial equilibrium E_0

The first simulation investigates the trivial equilibrium point $E_0(0,0,0)$, representing the extinction of all populations. Using the parameter values in Set 1 of Table 2, the condition $r < z_1(1-e)$ is satisfied, which guarantees that E_0 is locally asymptotically stable, consistent with Theorem 3.4. Numerical results in Figure 1 show that all populations decay to zero for different fractional orders $\alpha \in [0.7, 1]$. Specifically, Figures 1(a) and 1(b) depict the rapid decay of the prey and susceptible predator populations, respectively, while Figure 1(c) shows the corresponding decline of the infected predator population. The collective trajectory of this extinction process is further illustrated in the phase portrait of Figure 1(d).

This scenario corresponds to an ecosystem where intensive harvesting overwhelms the natural reproductive capacity of the prey. When the prey cannot sustain its population, both susceptible and infected predators eventually perish due to food scarcity. The inequality $r < z_1(1-e)$ reflects this ecological imbalance: high harvesting and limited accessible refuge $(1-e)$ drive the system toward extinction.

From a dynamical point of view, the fractional order α modulates the memory effect of the system. As α increases toward one, trajectories converge to the extinction state more rapidly, mimicking a fast ecological response with little memory of past population states. This is evident in the steeper initial declines shown in Figures 1(a-c) for $\alpha = 1$. Conversely, when α decreases (e.g., $\alpha = 0.7$), the convergence becomes slower, indicating that long ecological memory delays the collapse of populations even under unfavorable conditions. Thus, smaller α values represent ecosystems where past population conditions continue to influence the present, slightly buffering the rate of decline but not preventing eventual extinction.

Simulation 2: Predator-free equilibrium point E_1

The second simulation examines the predator-free equilibrium E_1, in which the prey persists while both susceptible and infected predators go extinct. Using the parameter values in Set 2 of Table 2, the condition $r > z_1(1-e)$ is satisfied, ensuring the existence of E_1, in agreement with Theorem 3.5. Numerical simulations in Figure 2 show that prey populations stabilize at a positive equilibrium, whereas both predator classes decline to zero for various fractional orders $\alpha \in [0.7, 1]$. Specifically, the time series in Figure 2(a) shows the prey population converging to its steady state, while Figures 2(b) and 2(c) illustrate the decline of the susceptible and infected predator

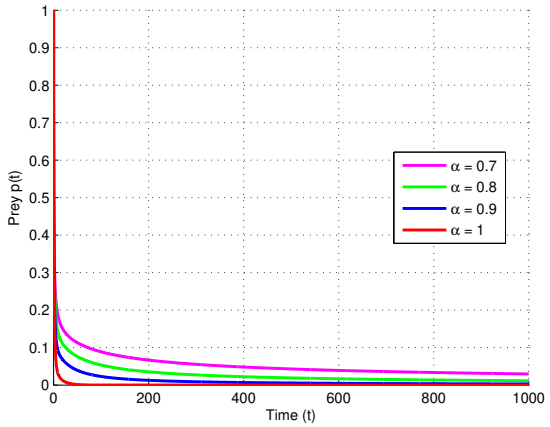

(a) Time series of the prey population (p).

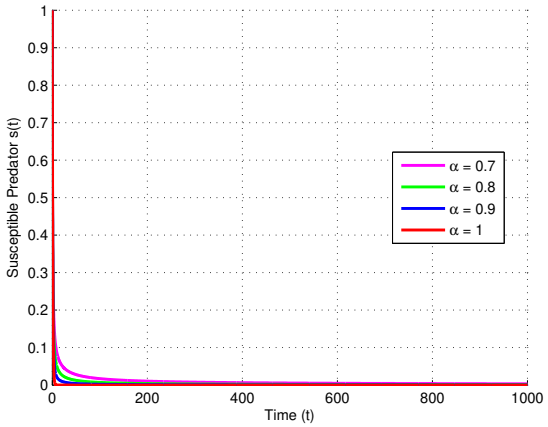

(b) Time series of the susceptible predator population (s).

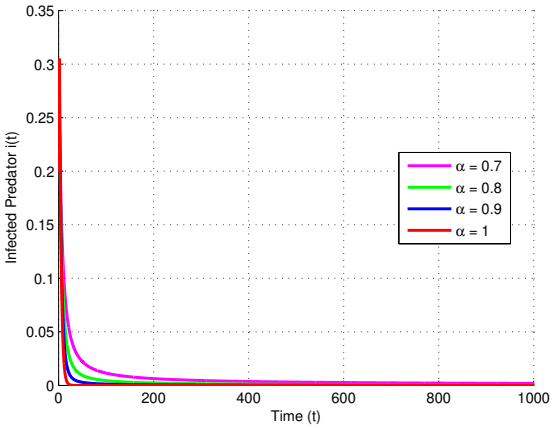

(c) Time series of the infected predator population (i).

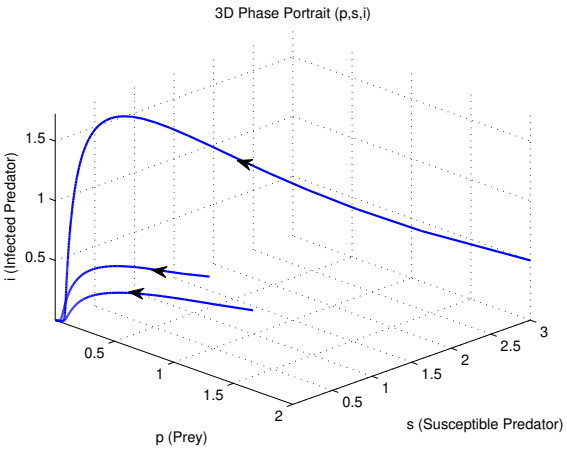

(d) Phase portrait of the system.

Figure 1. Simulation for parameter Set 1, showing convergence to the trivial equilibrium $E_0(0,0,0)$ for different fractional orders $\alpha = (0.7, 0.8, 0.9, 1)$: (a) Prey population, (b) Susceptible predator population, (c) Infected predator population, and (d) Phase portrait the model's solutions when $\alpha = 0.9$.

populations, respectively. The phase portrait in Figure 2(d) visualizes the system's trajectory towards the predator-free equilibrium on the prey axis.

This scenario represents an ecological system where the prey population can recover despite continuous harvesting, but predators cannot sustain themselves because their food source (prey) remains at a density too low to offset natural mortality and harvesting losses. The inequality $r > z_1(1-e)$ indicates that prey growth exceeds harvesting pressure, allowing prey survival even in the absence of predators. However, since prey abundance does not reach the level needed to support predator reproduction, both predator classes die out.

From a fractional-order perspective, the value of α governs the speed of ecological adjustment. For α close to one (e.g., $\alpha = 1$), the predator extinction occurs rapidly, and the prey quickly settles at its steady-state density, as seen in the sharp transitions in Figures 2(a-c). When α decreases (e.g., $\alpha = 0.7$), the trajectories exhibit slower convergence, with longer transients before reaching equilibrium. Ecologically, this implies that systems with stronger memory (smaller α) retain the influence of past predator–prey interactions longer, delaying predator extinction and prey stabilization. In contrast, when memory fades quickly (larger α), the populations respond more immediately to current conditions, leading to faster stabilization.

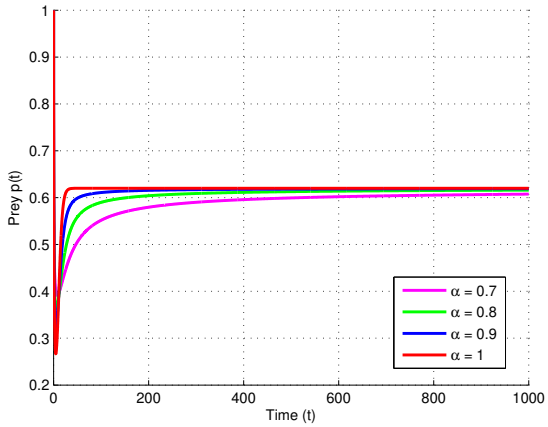

(a) Time series of the prey population (p).

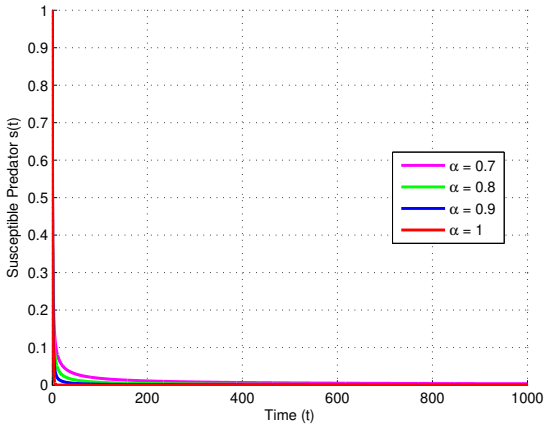

(b) Time series of the susceptible predator population (s).

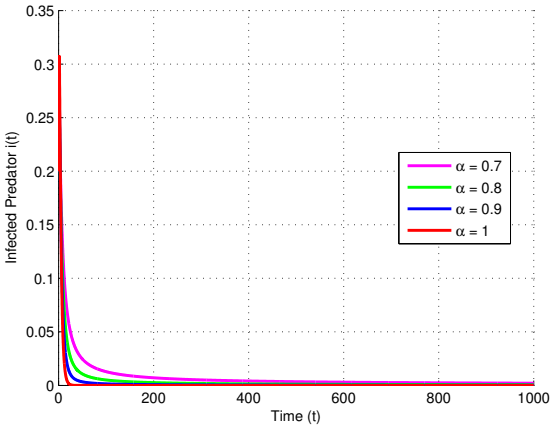

(c) Time series of the infected predator population (i).

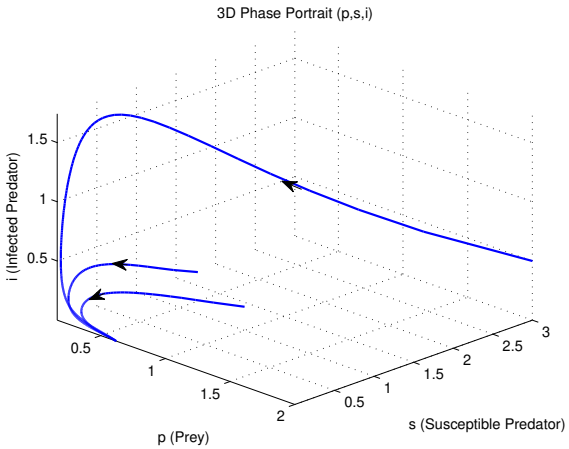

(d) Phase portrait converging to E_1 on the prey axis.

Figure 2. Simulation for parameter Set 2, showing convergence to the predator-free equilibrium E_1 for different fractional orders $\alpha = (0.7, 0.8, 0.9, 1)$: (a) Prey population, (b) Susceptible predator population, (c) Infected predator population, and (d) Phase portrait the model's solutions when $\alpha = 0.9$.

Simulation 3: Susceptible predator-free equilibrium E_2

The third simulation investigates the susceptible predator-free equilibrium E_2, where prey coexist with infected predators, while susceptible predators are driven to extinction. Using the parameter values in Set 3 of Table 2, the condition $c\nu_i > \gamma h$ is satisfied, confirming the existence of E_2 as established in Theorem 3.6. The numerical results in Figure 3 show that trajectories converge to E_2 for all tested fractional orders $\alpha \in [0.7, 1]$. Specifically, Figure 3(a) shows the stabilization of the prey population, Figure 3(b) demonstrates the extinction of the susceptible predator, and Figure 3(c) confirms the persistence of the infected predator at a low level. The phase portrait in Figure 3(d) illustrates the system's convergence to the equilibrium in the p-i plane.

This equilibrium illustrates an ecological state in which disease dynamics regulate the predator population. The infection reduces the predation efficiency of predators, allowing the prey to persist at moderate density. However, the infected predators can still maintain a small but stable population because their feeding activity, though reduced, is sufficient to balance mortality. The susceptible predators, which face higher competition and

disease transmission pressure, gradually disappear. Thus, the disease acts as a natural control mechanism that prevents predator overexploitation of prey.

From the viewpoint of fractional dynamics, the order α influences how the system responds to these competing processes of predation and infection. At higher α values (close to 1), the approach to equilibrium is faster, reflecting an ecosystem that rapidly adjusts to the new balance between disease and predation, as seen in the quick stabilization in Figures 3(a) and 3(c). For smaller α, the memory of past predator–prey interactions introduces inertia into the system: infection effects accumulate over time, and the transition toward equilibrium becomes smoother and more gradual. This suggests that long ecological memory can moderate fluctuations caused by disease transmission, promoting a more buffered coexistence between prey and infected predators.

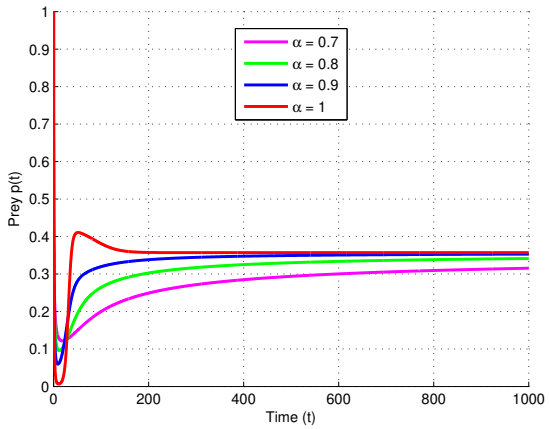

(a) Time series of the prey population (p).

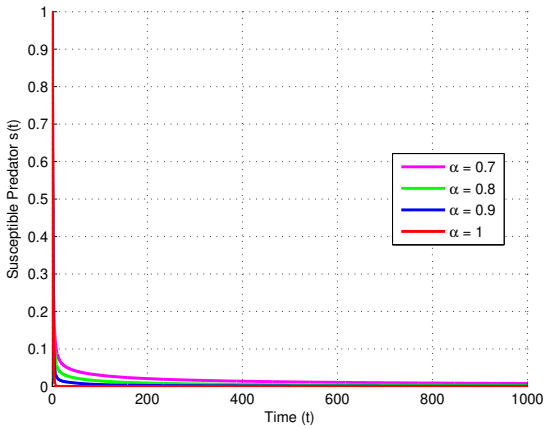

(b) Time series of the susceptible predator population (s).

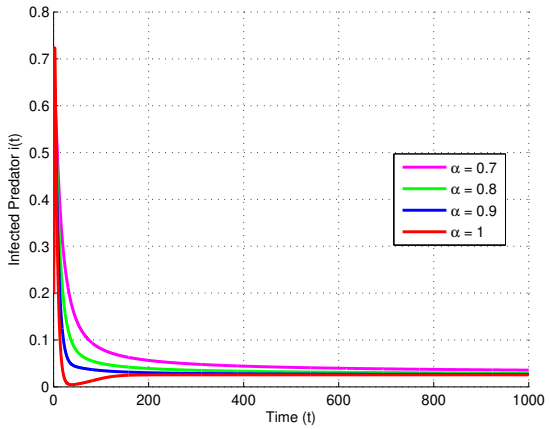

(c) Time series of the infected predator population (i).

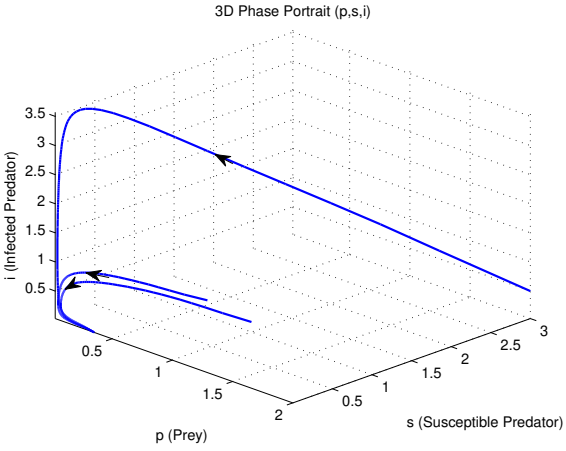

(d) Phase portrait in the p-i plane.

Figure 3. Simulation for parameter Set 3, showing convergence to the susceptible predator-free equilibrium E_2 for different fractional orders $\alpha = (0.7, 0.8, 0.9, 1)$: (a) Prey population stabilizes, (b) Susceptible predator population declines to zero, (c) Infected predator population persists, and (d) Phase portrait.

Simulation 4: Disease-free equilibrium E_3

The fourth simulation focuses on the disease-free equilibrium E_3, where prey coexist with healthy predators, while infected predators are eliminated. Using the parameter values in Set 4 of Table 2, the condition $c\nu > (d + z_2)h$

is fulfilled, confirming the existence of E_3 as predicted by Theorem 3.7. Numerical results in Figure 4 show that all trajectories converge to E_3 for different fractional orders $\alpha \in [0.7, 1]$. Specifically, Figure 4(a) shows the stabilization of the prey population, Figure 4(b) illustrates the persistence of the susceptible predator population, and Figure 4(c) confirms the extinction of the infected predator. The phase portrait in Figure 4(d) visualizes the system's approach to the equilibrium in the p-s plane.

This equilibrium describes a healthy ecological system where the predation pressure is sufficient to suppress the spread of disease within the predator population. The susceptible predators dominate, while the infected class cannot survive due to competitive disadvantage and higher mortality. Meanwhile, the prey population stabilizes at a moderate level, as continuous predation prevents excessive growth. The condition $c\nu > (d + z_2)h$ reflects an energetically efficient predator population capable of maintaining itself through consistent feeding, while harvesting and mortality remain balanced.

From the viewpoint of fractional dynamics, the order α influences the damping characteristics of the oscillatory behavior. For α approaching one, the system rapidly stabilizes after minor fluctuations, indicating a highly responsive ecological interaction with minimal memory of past states, as seen in the quick convergence in Figures 4(a-c). As α decreases, the trajectories exhibit weaker damping and longer-lasting oscillations before reaching equilibrium, revealing that ecological memory can sustain short-term population fluctuations. This suggests that when past interactions are retained (smaller α), the system temporarily experiences predator–prey cycles before eventually stabilizing, illustrating how memory prolongs but does not destabilize the return to equilibrium.

Simulation 5: Interior coexistence equilibrium E^*

The fifth simulation considers the interior coexistence equilibrium E^*, where prey, susceptible predators, and infected predators coexist in a dynamically balanced state. Using the parameter values in Set 5 of Table 2, the stability conditions $\varphi_1 > 0$, $\varphi_3 > 0$, and $\varphi_1\varphi_2 > \varphi_3$ are satisfied, confirming the local stability of E^* in agreement with Theorem 3.8. Numerical results presented in Figure 5 demonstrate that all population densities converge to positive steady states for different fractional orders $\alpha \in [0.7, 1]$. Specifically, Figures 5(a), 5(b), and 5(c) show the stabilization of prey, susceptible predator, and infected predator populations, respectively, while Figure 5(d) displays the three-dimensional phase portrait of their coexistence.

This equilibrium represents a fully interacting ecosystem in which prey persistence, predation, and disease transmission reach a natural balance. Predation pressure controls prey overgrowth, while the disease limits the dominance of healthy predators, preventing them from overexploiting the prey population. The infected predators, in turn, reduce the intensity of predation due to their lower hunting efficiency, which provides a protective feedback to the prey population. This bidirectional interaction forms a self-regulating loop that maintains all species at sustainable levels. The fractional order α adds an additional ecological layer to this balance. For higher α values (close to one), the populations quickly settle into steady coexistence, representing an ecosystem that adapts swiftly to perturbations with minimal memory of past interactions, as seen in the rapid convergence in Figures 5(a-c). When α decreases, memory effects become stronger, and the trajectories exhibit slower convergence with mild oscillatory behavior before stabilization. This behavior suggests that ecological memory smooths the adjustment among species: past predation and infection events influence current population growth, creating a more resilient but slower-reacting coexistence. Therefore, the fractional model captures how inherited ecological experiences such as lingering effects of disease or predation avoidance behavior can sustain the long-term coexistence of all interacting populations.

To provide a quantitative comparison of how the fractional order α affects system dynamics, an additional analysis was performed using the parameter values from Set 5 in Table 2. Figure 6 illustrates the relationship between α and the time required for the prey population to reach 95% of its equilibrium value (T_{95}). A clear decreasing trend is observed: as α increases from 0.7 to 1.0, the system reaches equilibrium more rapidly. This result confirms that higher α values, corresponding to weaker memory, accelerate the damping of oscillations, whereas smaller α values, representing stronger ecological memory, slow the convergence toward equilibrium. Ecologically, this means that when the system retains longer memory of past interactions, populations adjust more gradually to perturbations, delaying the approach to stability but contributing to smoother ecological transitions.

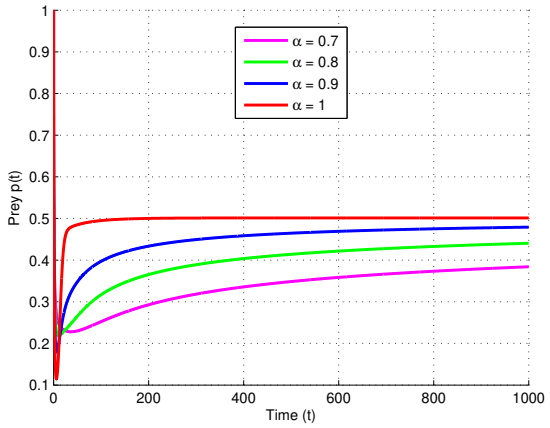

(a) Time series of the prey population (p).

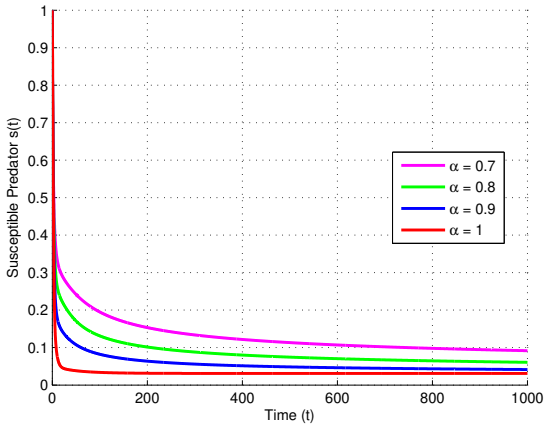

(b) Time series of the susceptible predator population (s).

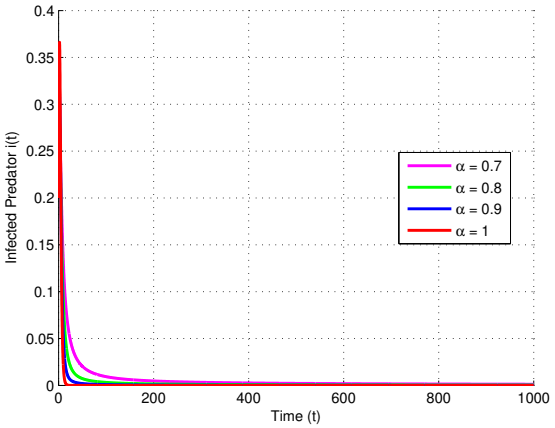

(c) Time series of the infected predator population (i).

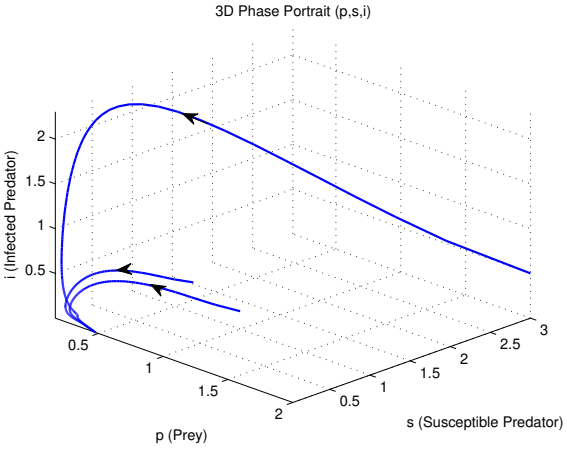

(d) Phase portrait in the p-s plane.

Figure 4. Simulation for parameter Set 4, showing convergence to the disease-free equilibrium E_3 for different fractional orders α: (a) Prey population stabilizes, (b) Susceptible predator population persists, (c) Infected predator population declines to zero, and (d) Phase portrait.

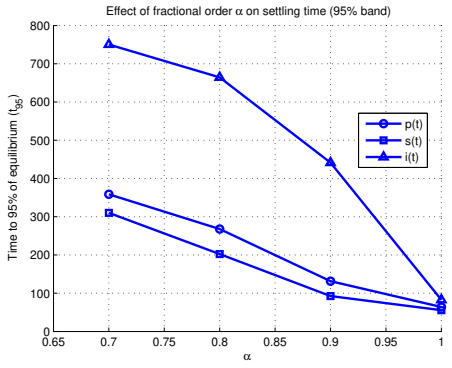

Figure 6. Quantitative relationship between the fractional order α and the time required for the prey population to reach 95% of its equilibrium value (T_{95}) using the parameter set 5. The decreasing trend indicates that larger α values lead to faster convergence, while smaller α (stronger memory) slow down the stabilization process.

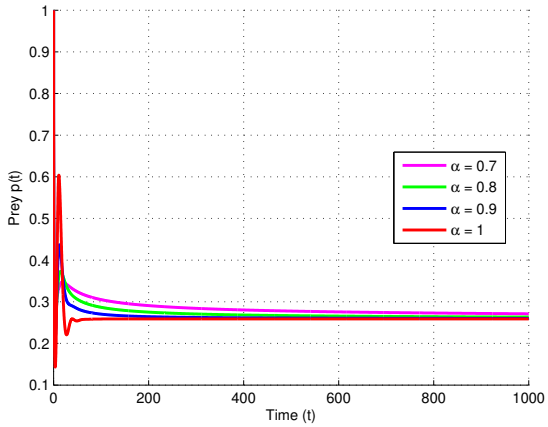

(a) Time series of the prey population (p).

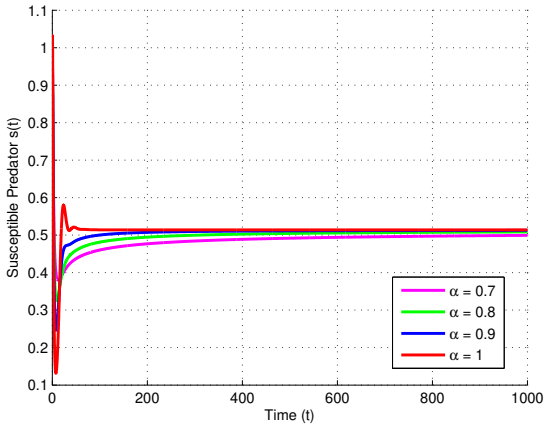

(b) Time series of the susceptible predator population (s).

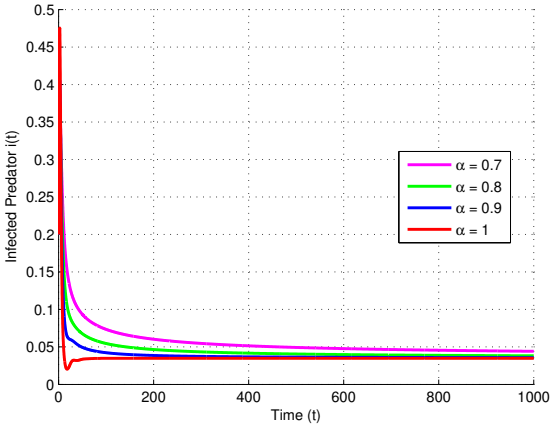

(c) Time series of the infected predator population (i).

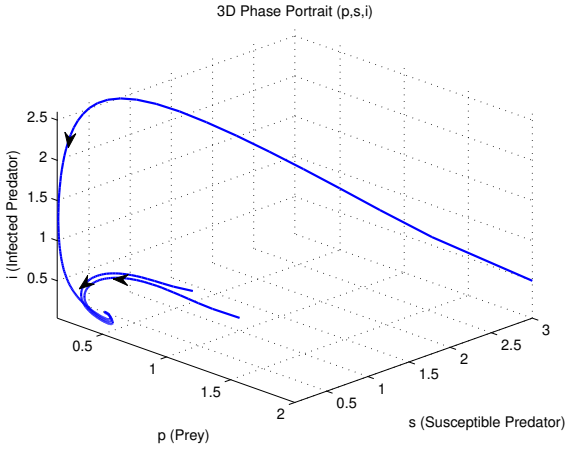

(d) Phase portrait of the coexistence equilibrium.

Figure 5. Simulation of the interior coexistence equilibrium E^* using parameter Set 5 for different fractional orders α: (a) Prey population stabilizes, (b) Susceptible predator population persists, (c) Infected predator population persists, and (d) Phase portrait.

Simulation 6: Effect of refuge and memory on stability

The final simulation investigates how the refuge proportion e and the fractional order α jointly affect the stability of the coexistence equilibrium. Using the parameter values in Set 6 of Table 2, Figure 7 presents the dynamics for different refuge levels at $\alpha = 1$, while Figure 8 explores the effect of memory ($\alpha < 1$) at a fixed refuge level.

At the integer order $\alpha = 1$, Figure 7 shows that when the refuge is high ($e = 0.8$), the system loses stability and exhibits oscillatory behavior (Figures 7(a) and 7(b)), indicating that excessive prey protection prevents effective predation and disrupts the ecological balance. However, when the refuge is reduced to $e = 0.2$ (Figures 7(c) and 7(d)) or $e = 0.1$ (Figures 7(e) and 7(f)), the system regains stability and all populations converge smoothly to coexistence. This demonstrates that moderate refuge provides enough safety for prey while still allowing sufficient predation to regulate population growth.

In contrast, Figure 8 reveals that even under a high-refuge condition ($e = 0.8$), the system can become stable when the fractional order is reduced from $\alpha = 1$ (Figures 8(a) and 8(b)) to $\alpha = 0.97$ (Figures 8(c) and 8(d)). The inclusion of fractional dynamics introduces ecological memory, meaning that present interactions are influenced by

past population states. This memory dampens abrupt oscillations and allows the system to recover stability that was lost in the purely integer-order case. Ecologically, this suggests that long term behavioral or physiological memory such as delayed predation responses or stress adaptation can counteract the destabilizing effects of excessive refuge, leading to a more resilient coexistence.

Taken together, Figures 7–8 provide a dedicated example in which varying the fractional order α leads to a *qualitative change* in system behavior: for the same high-refuge setting ($e = 0.8$), the coexistence equilibrium is unstable at $\alpha = 1$ but becomes stable at $\alpha = 0.97$. This stability switch directly demonstrates the distinctive role of ecological memory captured by fractional dynamics.

In addition to illustrating the stabilizing influence of ecological memory, Simulation 6 also serves as a qualitative sensitivity analysis. By systematically varying the refuge proportion (e) and the fractional order (α), the simulation reveals how small parameter changes can lead to marked differences in system behavior—from oscillatory instability to stable coexistence. This highlights the high sensitivity of the model to ecological protection mechanisms and memory effects, providing valuable insight into the robustness of the system's dynamics.

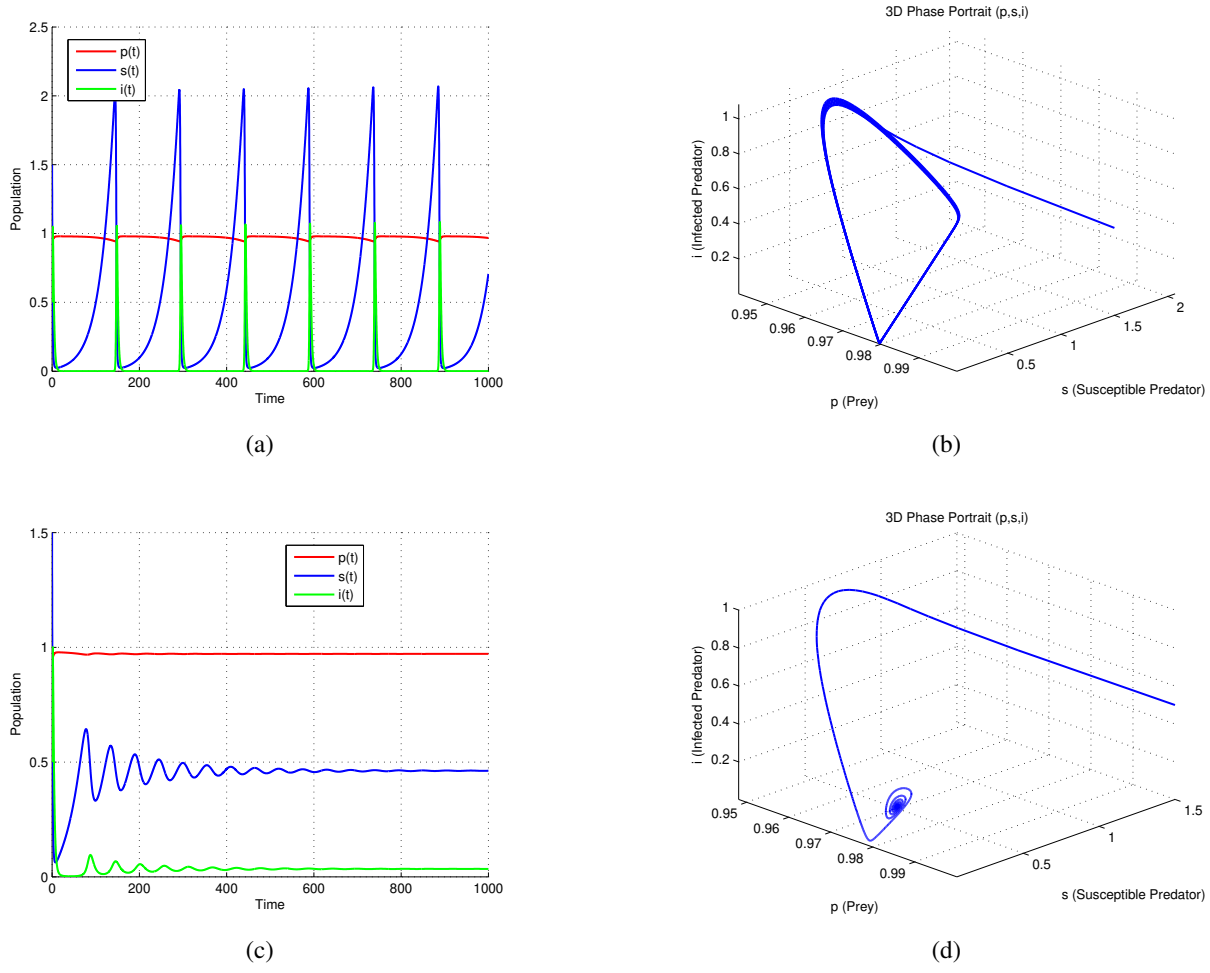

Figure 8. The graphs (a) and (b) illustrate the time series and phase portrait of the model's solutions when $\alpha = 1$, while the graphs(c) and (d) illustrate the time series and phase portrait of the model's solutions when $\alpha = 0.97$

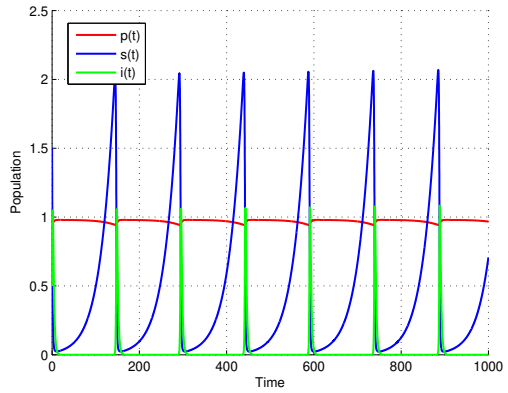

(a)

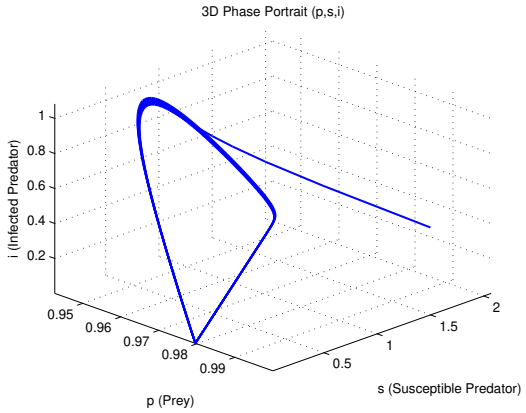

(b)

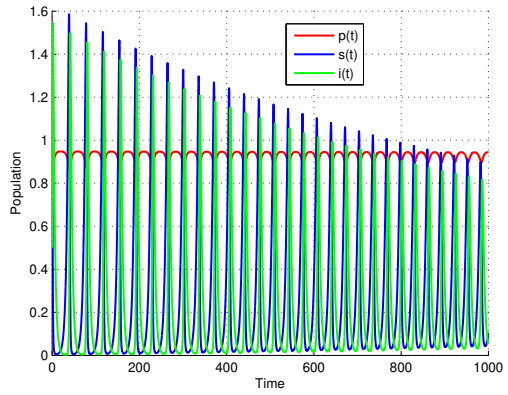

(c)

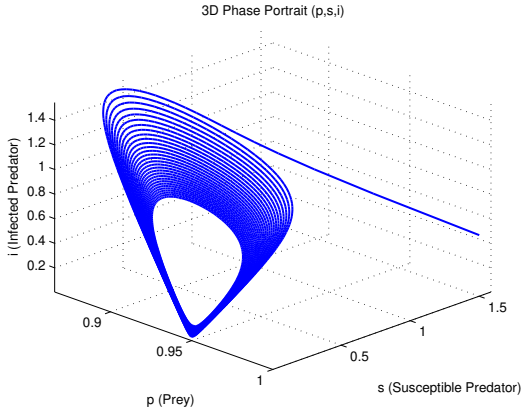

(d)

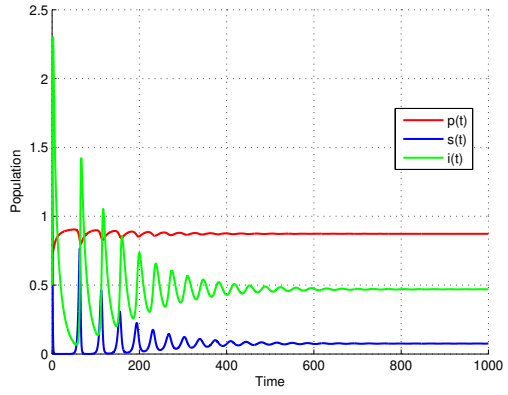

(e)

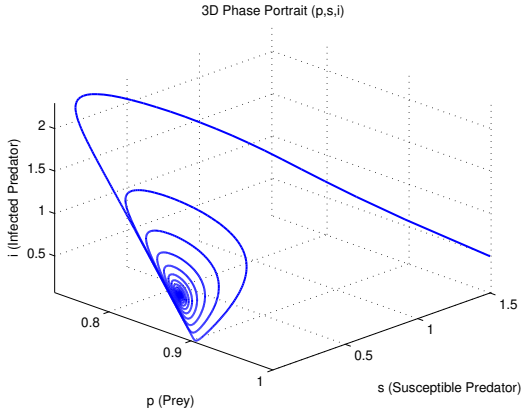

(f)

Figure 7. The dynamical behavior of the model system is analyzed for varying values of prey refuge and with fear set to $f = 0$. The graphs (a) and (b) illustrate the time series and phase portrait of the model's solutions for high refuge $e = 0.8$, the graphs (c) and (d) present the time series and phase portrait for moderate refuge $e = 0.2$, whereas the graphs (e) and (f) present the time series and phase portrait for low refuge $e = 0.1$.

5. Conclusions

This paper proposed and analyzed a fractional-order eco-epidemiological model that integrates fear effects, predator disease, and harvesting. The existence, uniqueness, and boundedness of the solutions were established, and the local stability of all feasible equilibria was examined. Numerical simulations confirmed the analytical results and illustrated how key ecological parameters influence the system's dynamic behavior.

The findings reveal that fear effects enhance prey persistence by reducing predation pressure, whereas excessive harvesting can drive predator extinction. Introducing the fractional derivative incorporates ecological memory into the system, substantially affecting the transient dynamics and stability. The fractional order α represents the degree of ecological memory, reflecting long-term stress responses or adaptive behaviors that influence population recovery and coexistence. These insights demonstrate how memory processes shape ecological resilience and link fractional calculus with biological interpretation in predator–prey–disease systems.

Simulation 6 further illustrates this property: small changes in the fractional order (α) can induce a qualitative shift in system stability. For the same parameter set, the coexistence equilibrium that is unstable at $\alpha = 1$ becomes stable at $\alpha = 0.97$. This finding highlights the distinctive ability of fractional dynamics to capture ecological memory and its stabilizing influence in complex interactions.

Model Limitations and Future Directions

Several simplifying assumptions should be noted. The disease transmission is modeled only within the predator population using a simple SI structure, while more complex frameworks such as SIR or SEIR are not considered. Harvesting is treated as constant, ignoring seasonal or stochastic variability commonly observed in natural ecosystems. The refuge effect is represented as a proportional term without spatial or behavioral adaptation. Future studies could extend the model by including time delays, age or stage structure, spatially explicit refuge, or empirical parameterization from field data to enhance ecological realism.

Additionally, management oriented extensions could further broaden the model's applicability. Optimizing the harvesting rates (z_1, z_2) through optimal control formulations may help balance biodiversity conservation and economic yield. Incorporating climate related drivers such as temperature dependent disease transmission or predator behavioral changes could also elucidate how environmental fluctuations interact with ecological memory. Together, these developments would extend the fractional framework from theoretical exploration toward practical tools for sustainable ecosystem management.

Appendix

Coefficient of p^* in equation (4)

$$
\begin{aligned}
A &= \gamma - (d + z_2) \\
B &= c(\nu - \nu_i)(1 - e) \\
C_0 &= -r + z_1(1-e) + z_1(1-e)fA - \nu_i(1-e)d - \nu_i(1-e)z_2 \\
&\quad - \nu_i(1-e)fAd - \nu_i(1-e)fAz_2 + \nu(1-e)\gamma + \nu(1-e)\gamma fA \\
C_1 &= -3hr(1-e) + r + rfA + 2\nu(1-e)\gamma h(1-e) \\
&\quad + 2\nu(1-e)^2\gamma fAh + \nu(1-e)\gamma fB - \nu(1-e)^2 c\nu_i \\
&\quad - f\nu(1-e)^2 c\nu_i A + z_1(1-e)^2 2h + \nu_i(1-e)^2 c\nu \\
&\quad - \nu_i(1-e)^2 dh - \nu_i(1-e)^2 z_2 h + \nu_i(1-e)^2 c\nu fA \\
&\quad - \nu_i(1-e)^2 dhfA - \nu_i(1-e)^2 z_2 hfA - \nu_i(1-e)^2 dh \\
&\quad - \nu_i(1-e)^2 z_2 h - \nu_i(1-e)^2 dhfA - \nu_i(1-e)^2 z_2 hfA \\
&\quad - \nu_i(1-e)dfB - \nu_i(1-e)z_2 fB + z_1(1-e)^2 2hfA
\end{aligned}
$$

$$
\begin{aligned}
&+ z_1(1-e)fB + z_1(1-e)^2hfA + z_1(1-e)^2h \\
C_2 = &-3rh^2(1-e)^2 + 2rh(1-e) + 2rhfA(1-e) + rh(1-e) \\
&+ rh(1-e)fA + rfB + \nu\gamma h^2(1-e)^3 + \nu\gamma h^2 fA(1-e)^3 \\
&+ h(1-e)^2\nu\gamma fB - h\nu(1-e)^3 c\nu_i - \nu(1-e)^3 c\nu_i hfA \\
&- \nu(1-e)^2 c\nu_i fB + \nu_i(1-e)^3 c\nu h - \nu_i(1-e)^3 dh^2 \\
&- \nu_i z_2(1-e)^3h^2 + \nu_i(1-e)^3 c\nu hfA - \nu_i d(1-e)^3 fAh^2 \\
&- \nu_i(1-e)^3 z_2 fAh^2 + \nu_i(1-e)^2 c\nu fB - \nu_i(1-e)^2 dhfB \\
&- \nu_i(1-e)^2 z_2 hfB + z_1h^2(1-e)^3 + z_1h^2(1-e)^3 fA \\
&+ z_1(1-e)^2 2(1-e)h^2 + z_1(1-e)^3 2fAh^2 + z_1(1-e)^2 2hfB \\
C_3 = &-rh^3(1-e)^3 + rh^2(1-e)^2 + rfAh^2(1-e)^2 + 2rh^2(1-e)^2 \\
&+ 2rh^2 fA(1-e)^2 + 2rhfB(1-e) + z_1h^3(1-e)^4 \\
&+ z_1h^2(1-e)^4 hfA + z_1h^2(1-e)^3 fB \\
C_4 = &\, rh^3(1-e)^3 + rh^3 fA(1-e)^3 + rh^2 fB(1-e)^2
\end{aligned}
$$

Acknowledgement

The authors acknowledge the support of Indonesian Education Scholarship[ID: 202209090769], Center for Higher Education Funding and Assessment, and Indonesian Endowment Fund for Education.

REFERENCES

1. A.U. Igamberdiev and J.E. Brenner, *Mathematics in biological reality: the emergence of natural computation in living systems*, Biosystems, vol. 204, pp. 104395, 2021.
2. K. Singh, T. Singh, L.N. Mishra, R. Dubey, and L. Rathour, *A brief review of predator-prey models for an ecological system with a different type of behaviors*, Korean Journal of Mathematics, vol. 32, no. 3, pp. 381–406, 2024.
3. N.H. Fakhry and R.K. Naji, *The dynamic of an eco-epidemiological model involving fear and hunting cooperation*, Commun. Math. Biol. Neurosci., vol. 2023, pp. 1–33, 2023.
4. S. Zhang, S. Yuan, and T. Zhang, *Dynamic analysis of a stochastic eco-epidemiological model with disease in predators*, Studies in Applied Mathematics, vol. 149, no. 1, pp. 5–42, 2022.
5. V. Kumar, N. Kumari, and R.P. Agarwal, *Spatiotemporal dynamics and Turing patterns in an eco-epidemiological model with cannibalism*, Results in Control and Optimization, vol. 9, pp. 100183, 2022.
6. S. Biswas, B. Ahmad, and S. Khajanchi, *Exploring dynamical complexity of a cannibalistic eco-epidemiological model with multiple time delay*, Mathematical Methods in the Applied Sciences, vol. 46, no. 4, pp. 4184–4211, 2023.
7. S. Biswas, S. Samanta, and J. Chattopadhyay, *A cannibalistic eco-epidemiological model with disease in predator population*, Journal of Applied Mathematics and Computing, vol. 57, pp. 161–197, 2018.
8. A. Divya, M. Sivabalan, A. Ashwin, and M.S. Pradeep, *Dynamics of a Crowley-Martin functional response eco-epidemiological model with prey refuge and disease in the prey*, AIP Conference Proceedings, 2024.
9. M. Khan, P. Sen, and S. Samanta, *Stability and bifurcation analysis of an eco-epidemiological model with prey refuge*, Nonlinear Studies, vol. 431, no. 1, pp. 183–209, 2024.
10. A.K. Pal, A. Bhattacharyya, and S. Pal, *Study of delay induced eco-epidemiological model incorporating a prey refuge*, Filomat, vol. 36, no. 2, pp. 557–578, 2022.
11. D. Das and T.K.K. Kar, *Feedback control and its impact on generalist predator–prey system with prey harvesting*, Nonlinear Analysis: Modelling and Control, vol. 24, no. 5, pp. 718–732, 2019.
12. C. Zhang, S. Liu, J. Huang, and W. Wang, *Stability and Hopf bifurcation in an eco-epidemiological system with the cost of anti-predator behaviors*, Mathematical Biosciences and Engineering, pp. 8146–8161, 2023.
13. A.K. Pal, A. Bhattacharyya, A. Mondal, and S. Pal, *Qualitative analysis of an eco-epidemiological model with a role of prey and predator harvesting*, Zeitschrift für Naturforschung A, vol. 77, no. 7, pp. 629–645, 2022.
14. K. Hassan, A. Mustafa, M. Hama, and S. Pal, *An eco-epidemiological model incorporating harvesting factors*, Symmetry, vol. 13, no. 11, pp. 2179, 2021.
15. H. Mollah and S. Sarwardi, *Mathematical modeling and bifurcation analysis of a delayed eco-epidemiological model with disease in predator and linear harvesting*, International Journal of Modelling and Simulation, pp. 1–21, 2024.
16. S.K. Sasmal, Y. Kang, and J. Chattopadhyay, *Intra-specific competition in predator can promote the coexistence of an eco-epidemiological model with strong Allee effects in prey*, BioSystems, vol. 137, pp. 34–44, 2015.

17. M. Sarkar, A. Mondal, A. Bhattacharyya, and A.K. Pal, *A Lesli-Gower type predator-prey model with Allee effect and disease in predator*, Discontinuity, Nonlinearity, and Complexity, vol. 14, no. 1, pp. 39–61, 2025.
18. B.K. Dasa, N. Santraa, and G. Samantaa, *Exploring dynamics of predator-prey interactions: fear, toxicity, carry over and environmental fluctuations*, Filomat, vol. 38, no. 31, pp. 11061–11083, 2024.
19. S.N. Afiyah, Fatmawati, and Windarto, *Dynamical analysis of a Leslie-Gower predator-prey model with Holling type IV functional response incorporating fear and Allee effect*, AIP Conference Proceedings, vol. 3302, no. 1, 2025.
20. H. Chen and C. Zhang, *Dynamic analysis of a Leslie–Gower-type predator–prey system with the fear effect and ratio-dependent Holling III functional response*, Nonlinear Analysis: Modelling and Control, vol. 27, no. 5, pp. 904–926, 2022.
21. A. Sha and J. Chattopadhyay, *Dynamical study of fear effect in prey–predator model with disease in predator*, Journal of Biological Systems, vol. 31, no. 4, pp. 1319–1340, 2023.
22. A.J. Kashyap and H.K. Sarmah, *Complex dynamics in a predator–prey model with fear affected transmission*, Differential Equations and Dynamical Systems, pp. 1–32, 2024.
23. K. Sarkar and S. Khajanchi, *An eco-epidemiological model with the impact of fear*, Chaos: An Interdisciplinary Journal of Nonlinear Science, vol. 32, no. 8, 2022.
24. L. Teckentrup, V. Grimm, S. Kramer-Schadt, and F. Jeltsch, *Community consequences of foraging under fear*, Ecological Modelling, vol. 383, pp. 80–90, 2018.
25. S.K. Sasmal, *Population dynamics with multiple Allee effects induced by fear factors–A mathematical study on prey-predator interactions*, Applied Mathematical Modelling, vol. 64, pp. 1–14, 2018.
26. U. Ghosh, A.A. Thirthar, B. Mondal, and P. Majumdar, *Effect of fear, treatment, and hunting cooperation on an eco-epidemiological model: Memory effect in terms of fractional derivative*, Iranian Journal of Science and Technology, Transactions A: Science, vol. 46, no. 6, pp. 1541–1554, 2022.
27. J. Liu, B. Liu, P. Lv, and T. Zhang, *An eco-epidemiological model with fear effect and hunting cooperation*, Chaos, Solitons & Fractals, vol. 142, pp. 110494, 2021.
28. A. Chatterjee, M.A. Abbasi, E. Venturino, J. Zhen, and M. Haque, *A predator–prey model with prey refuge: Under a stochastic and deterministic environment*, Nonlinear Dynamics, pp. 1–27, 2024.
29. S. Pal, F. Al Basir, and S. Ray, *Impact of cooperation and intra-specific competition of prey on the stability of prey–predator models with refuge*, Mathematical and Computational Applications, vol. 28, no. 4, pp. 88, 2023.
30. Z.I.A. Manaf and M.H. Mohd, *The effects of varying predator dispersal strength on prey-predator dynamics with refuge process*, Malaysian Journal of Fundamental and Applied Sciences, vol. 19, no. 5, pp. 791–803, 2023.
31. F.M. Hilker and E. Liz, *Threshold harvesting as a conservation or exploitation strategy in population management*, Theoretical Ecology, vol. 13, pp. 519–536, 2020.
32. A. Asunsolo-Rivera, E. Lester, T. Langlois, B. Vaughan, M. I.McCormick, S. D. Simpson, and M. G. Meekan, *Behaviour of mesopredatory coral reef fishes in response to threats from sharks and humans*, Scientific Reports, vol. 13, no. 1, pp. 6714, 2023.
33. D.S. Glazier, *Scaling species interactions: Implications for community ecology and biological scaling theory*, Academia Biology, vol. 1, no. 4, 2023.
34. S. Rossi, *Fishing and overfishing—sustainable harvest of the sea*, in SDG 14: Life below water: A machine-generated overview of recent literature, Cham: Springer International Publishing, pp. 207–325, 2022.
35. B. Daşbaş, *Stability analysis of mathematical model including pathogen-specific immune system response with fractional-order differential equations*, Computational and Mathematical Methods in Medicine, pp. 1–10, 2018.
36. H.A.A. El-Saka, A.A.M. Arafa, and M.I. Gouda, *Dynamical analysis of a fractional SIRS model on homogenous networks*, Advances in Difference Equations, pp. 1–15, 2019.
37. S. Paul, S. Mahato, A. Mahata, S.K. Mahato, S. Mukherjee, and B. Roy, *Analysis of an imprecise fractional-order eco-epidemiological model with various forms of prey refuges and predator harvesting*, Brazilian Journal of Physics, vol. 55, no. 1, pp. 12, 2025.
38. C. Song and N. Li, *Dynamic analysis and bifurcation control of a delayed fractional-order eco-epidemiological migratory bird model with fear effect*, International Journal of Biomathematics, vol. 17, no. 3, pp. 2350022, 2024.
39. P. Sireeshadevi, *Dynamical behavior of an eco-epidemiological model incorporating Holling type-II functional response with prey refuge and constant prey harvesting*, Network Biology, vol. 14, no. 3, pp. 228, 2024.
40. I. Domínguez-Alemán, J.C. Hernández-Gómez, and F.J. Ariza-Hernández, *A predator-prey fractional model with disease in the prey species*, Mathematical Biosciences and Engineering, vol. 21, no. 3, pp. 3713–3741, 2024.
41. M. Moustafa, F.A. Abdullah, S. Shafie, and N.A. Amirsom, *Global stability of a fractional-order eco-epidemiological model with infected predator: Theoretical analysis*, Communications in Mathematical Biology and Neuroscience, 2023.
42. F. Li, B. Günay, K.S. Nisar, and M.S. Alharthi, *Incorporating fractional operators into interaction dynamics studies: An eco-epidemiological model*, Results in Physics, vol. 47, pp. 106385, 2023.
43. H.S. Panigoro, N. Anggriani, and E. Rahmi, *Understanding the role of intraspecific disease transmission and quarantine on the dynamics of eco-epidemiological fractional order model*, Fractal and Fractional, vol. 7, no. 8, pp. 610, 2023.
44. S.N. Afiyah, Fatmawati, Windarto, and A. Abidemi, *Dynamics of a fractional order harvested predator-prey model incorporating fear effect and refuge*, Statistics, Optimization & Information Computing, vol. 13, no. 4, pp. 1690–1713, 2025.
45. S. Olaniyi, F.M. Chuma, and S.F. Abimbade, *Asymptotic stability analysis of a fractional epidemic model for Ebola virus disease in Caputo sense*, Journal of the Nigerian Society of Physical Sciences, vol. 7, pp. 2304–2304, 2025.
46. A. Chatterjee, M.A. Abbasi, E. Venturino, J. Zhen, M. Haque, *A predator–prey model with prey refuge: under a stochastic and deterministic environment*, Nonlinear Dynamics, vol. 112, pp. 13667–13693, 2024.
47. B. Kumar, R.K. Sinha, *Dynamics of an eco-epidemic model with Allee effect in prey and disease in predator*, Computational and Mathematical Biophysics, vol. 11, pp. 20230108, 2023.
48. M. Moustafa, M.H. Mohd, A.I. Ismail, F.A. Abdullah, *Dynamical analysis of a fractional-order eco-epidemiological model with disease in prey population*, Advances in Difference Equations, vol. 2020 (1), pp. 48, 2020.

49. M. Mandal, S. Jana, S.K. Nandi, T.K. Kar, *Modelling and control of a fractional-order epidemic model with fear effect*, Energy, Ecology and Environment, vol. 5, pp. 421–432, 2020.
50. D. Barman, J. Roy, H. Alrabaiah, P. Panja, S.P. Mondal, S. Alam , *Impact of predator incited fear and prey refuge in a fractional order prey predator model*, Chaos, Solitons & Fractals, vol. 142, pp. 110420, 2021.
51. M.S. Islam, S. Hossain, S. Sarwardi, *Dynamical analysis of an eco-epidemic system with different forms of prey refuges and predator harvesting*, Discontinuity, Nonlinearity, and Complexity, vol. 13, pp. 95-112, 2024.
52. M Moustafa, FA Abdullah, S Shafie, *Dynamical behavior of a fractional-order prey–predator model with infection and harvesting*, Journal of Applied Mathematics and Computing, vol. 68, pp. 4777–4794, 2022.
53. C. Maji, *Impact of fear effect in a fractional-order predator–prey system incorporating constant prey refuge*, Nonlinear Dynamics, vol. 107, pp. 1329–1342, 2022.
54. S. Paul, S. Mahato, A. Mahata, S.K. Mahato, S. Mukherjee, B. Roy, *Analysis of an imprecise fractional-order eco-epidemiological model with various forms of prey refuges and predator harvesting*, Nonlinear Dynamics, vol. 55(2), pp. 12, 2025.
55. J. Cresson and A. Szafrańska, *Discrete and continuous fractional persistence problems—The positivity property and applications*, Communications in Nonlinear Science and Numerical Simulation, vol. 44, pp. 424–448, 2017.
56. Y. Li, Y.Q. Chen, and I. Podlubny, *Stability of fractional-order nonlinear dynamic systems: Lyapunov direct method and generalized Mittag–Leffler stability*, Computers & Mathematics with Applications, vol. 59, pp. 1810–1821, 2010.
57. C. Vargas-De-León, *Volterra-type Lyapunov functions for fractional-order epidemic systems*, Communications in Nonlinear Science and Numerical Simulation, vol. 24, pp. 75–85, 2015.
58. D.K. Almutairi, I.K. Argyros, K. Gdawiec, S. Qureshi, A. Soomro, K.H. Jamali, M. Alquran, and A. Tassaddiq, *Algorithms of predictor-corrector type with convergence and stability analysis for solving nonlinear systems*, AIMS Mathematics, vol. 9, pp. 32014–32044, 2024.